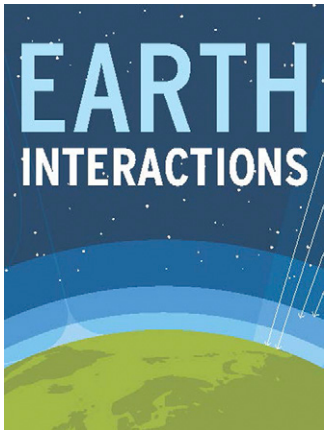

Copyright © 2016, Paper 20-013; 517 words, 0 Figures, 0 Animations, 1 Tables.
http://EarthInteractions.org

CORRIGENDUM

Ashley E. Van Beusekom,* Grizelle González, and Maria M. Rivera

USDA Forest Service International Institute of Tropical Forestry, Río Piedras, Puerto Rico

Received and in final form 8 May 2015

Figure 1 in "Short-term precipitation and temperature trends along an elevation gradient in Northeastern Puerto Rico" by Van Beusekom et al. (2015) was incorrect in the paper. The sites were incorrectly labeled and are corrected here in Table 1. The authors would like to thank Sheila Murphy (U.S. Geological Survey) for identifying this problem. Additionally, the station elevations reported in the paper were determined using differing methods that lead to slight inconsistencies in the elevations. To correct this, the elevations have been standardized using station *x*–*y* coordinates and elevation above mean sea level extracted from the U.S. Geological Survey 10-m DEM. Revised columns are shown in Table 1 here. The comparisons with the outside data source were reanalyzed using these locations and elevations, and the regressions of Sen's slopes of the trends versus elevation were recomputed using these elevations. The results shown in Figure 10 (no relationship between temperature trends and elevation) remain the same. The results shown in Figure 9 change slightly. The relationship for all months' precipitation with elevation should be

* Corresponding author address: Ashley E. Van Beusekom, SDA Forest Service International Institute of Tropical Forestry, Jardín Botánico Sur, 1201 Calle Ceiba, Río Piedras, Puerto Rico 00926.

E-mail address: ashley.vanbeusekom@gmail.com

DOI: 10.1175/EI-D-15-0044.1

Table 1. Revised columns for Table 1 from Van Beusekom et al. (2015).

Standardized elevation (m)	Map ID	Site ID	Site name
31	1	1	Las Cabezas Dry
4	2	4	Las Cabezas Wet
0	6	6	Palmas del Mar
3	5	7	Humacao
3	7	5	Sabana Seca
14	3	2	Ceiba Dry North
13	8	9	Ford
9	4	3	Ceiba Dry South
81	9	10	Saint Just
26	10	8	Jardin Botánico
226	11	13	Sabana 4
361	12	11	El Verde
525	13	12	Rio Grande
655	14	14	UPR Nido
778	16	15	Pico del Este Lower
792	17	16	El Toro
901	15	17	Mount Britton
1002	18	18	Pico del Este Upper
987	19	19	Pico del Oeste
1045	20	20	El Yunque

$y = (0.75 \times 10^{-4})x + 0.15$ with a p value of 0.126 for the slope and 0.001 for the intercept, with y as the change in mean daily precipitation per year (mm) and x as elevation (m). The relationship for driest months' precipitation with elevation should be $y = (2.05 \times 10^{-4})x + 0.10$ with a p value of 0.001 for the slope and 0.013 for the intercept, with y as the change in mean daily precipitation per year (mm) and x as elevation (m). These are approximately a 3% reduction from the reported slopes of increasing change of mean daily precipitation with elevation. The individual station trends do not change, just the magnitude of the increase of the trends with elevation.

REFERENCE

Van Beusekom, A. E., G. González, and M. M. Rivera, 2015: Short-term precipitation and temperature trends along an elevation gradient in northeastern Puerto Rico. *Earth Interact.*, **19**, doi:10.1175/EI-D-14-0023.1.

Earth Interactions is published jointly by the American Meteorological Society, the American Geophysical Union, and the Association of American Geographers. Permission to use figures, tables, and *brief* excerpts from this journal in scientific and educational works is hereby granted provided that the source is acknowledged. Any use of material in this journal that is determined to be "fair use" under Section 107 or that satisfies the conditions specified in Section 108 of the U.S. Copyright Law (17 USC, as revised by P.IL. 94-553) does not require the publishers' permission. For permission for any other from of copying, contact one of the copublishing societies.

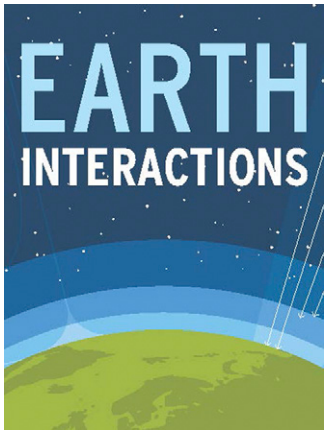

Copyright © 2015, Paper 19-003; 90,743 words, 10 Figures, 0 Animations, 4 Tables.
http://EarthInteractions.org

Short-Term Precipitation and Temperature Trends along an Elevation Gradient in Northeastern Puerto Rico

Ashley E. Van Beusekom,* Grizelle González, and Maria M. Rivera

USDA Forest Service International Institute of Tropical Forestry, Río Piedras, Puerto Rico

Received 27 March 2014; accepted 23 October 2014

ABSTRACT: As is true of many tropical regions, northeastern Puerto Rico is an ecologically sensitive area with biological life that is highly elevation dependent on precipitation and temperature. Climate change has the potential to increase the risk of losing endemic species and habitats. Consequently, it is important to explore the pattern of trends in precipitation and temperature along an elevation gradient. Statistical derivatives of a frequently sampled dataset of precipitation and temperature at 20 sites along an elevation gradient of 1000 m in northeastern Puerto Rico were examined for trends from 2001 to 2013 with nonparametric methods accounting for annual periodic variations such as yearly weather cycles. Overall daily precipitation had an increasing trend of around 0.1 mm day^{-1} yr^{-1}. The driest months of the annual dry, early, and late rainfall seasons showed a small increasing trend in the precipitation (around

* Corresponding author address: Ashley E. Van Beusekom, USDA Forest Service International Institute of Tropical Forestry, Jardín Botánico Sur, 1201 Calle Ceiba, Río Piedras, PR 00926.
E-mail address: ashley.vanbeusekom@gmail.com

DOI: 10.1175/EI-D-14-0023.1

0.1 mm day^{-1} yr^{-1}). There was strong evidence that precipitation in the driest months of each rainfall season increased faster at higher elevations (0.02 mm day^{-1} more increase for 100-m elevation gain) and some evidence for the same pattern in precipitation in all months of the year but at half the rate. Temperature had a positive trend in the daily minimum (around 0.02°C yr^{-1}) and a negative trend in the daily maximum whose size is likely an order of magnitude larger than the size of the daily minimum trend. Physical mechanisms behind the trends may be related to climate change; longer-term studies will need to be undertaken in order to assess the future climatic trajectory of tropical forests.

KEYWORDS: Tropics; Statistical techniques; Statistics; Seasonal variability; Trends

1. Introduction

Tropical ecosystems are widely recognized for their diversity of species that are highly dependent on climate, making them ecologically sensitive regions (Denslow 1987; Phillips and Gentry 1994; Vitousek 1998). Northeastern Puerto Rico (PR) is one such region. Recently, a series of regionwide studies have documented the wide distribution of microbe and animal characteristics (Cantrell et al. 2013; Richardson and Richardson 2013; Willig et al. 2013), soil dynamics (Ping et al. 2013; Silver et al. 2013), and vegetation properties (González and Luce 2013; Harris and Medina 2013; Weaver and Gould 2013). These distributions vary due to the climatic differences along the elevation gradient. Across the globe, projected climatic changes are expected to greatly change the distribution and diversity of species contained in tropical ecosystems (Halpin 1997; Scatena 1998).

However, it is not understood how these climatic changes will behave across an elevation gradient, and it is often assumed the spatial pattern of the climatic variables will stay the same in the future with climatic shifts occurring in a uniform proportional manner (precipitation) or uniform scalar manner (temperature) across elevation gradients (Enquist 2002; Hilbert et al. 2001; Wang et al. 2003). In this vein, there have been numerous studies published on the climatic trends in northeastern PR in totality (Burrowes et al. 2004; Comarazamy and González 2011; Greenland and Kittel 2002; Heartsill-Scalley et al. 2007) but not on the differences in the trends along an elevation gradient. Other studies have looked at existing climatic conditions along an elevation gradient (García-Martinó et al. 1996; Waide et al. 2013) but not at the trends in the climatic variables.

The objective of this study was to fill some of the existing knowledge gap by examining the short-term trends in the climatic variables of precipitation and temperature along an elevation gradient of 1000 m from 2001 to 2013. Furthermore, trends along the elevation gradient of wettest and driest months of each rainfall season and maximum and minimum in daily temperatures were investigated to explore in which aspects observed trends in overall precipitation and temperature were realized. Results from this study highlight the possibility of differing patterns of climate change across elevation gradients in tropical ecosystems as a whole.

2. Study area

PR is the smallest of the Greater Antilles island chain, located in the northeastern Caribbean Sea (17°45′N, 66°15′W) (Figure 1). PR follows the Caribbean weather

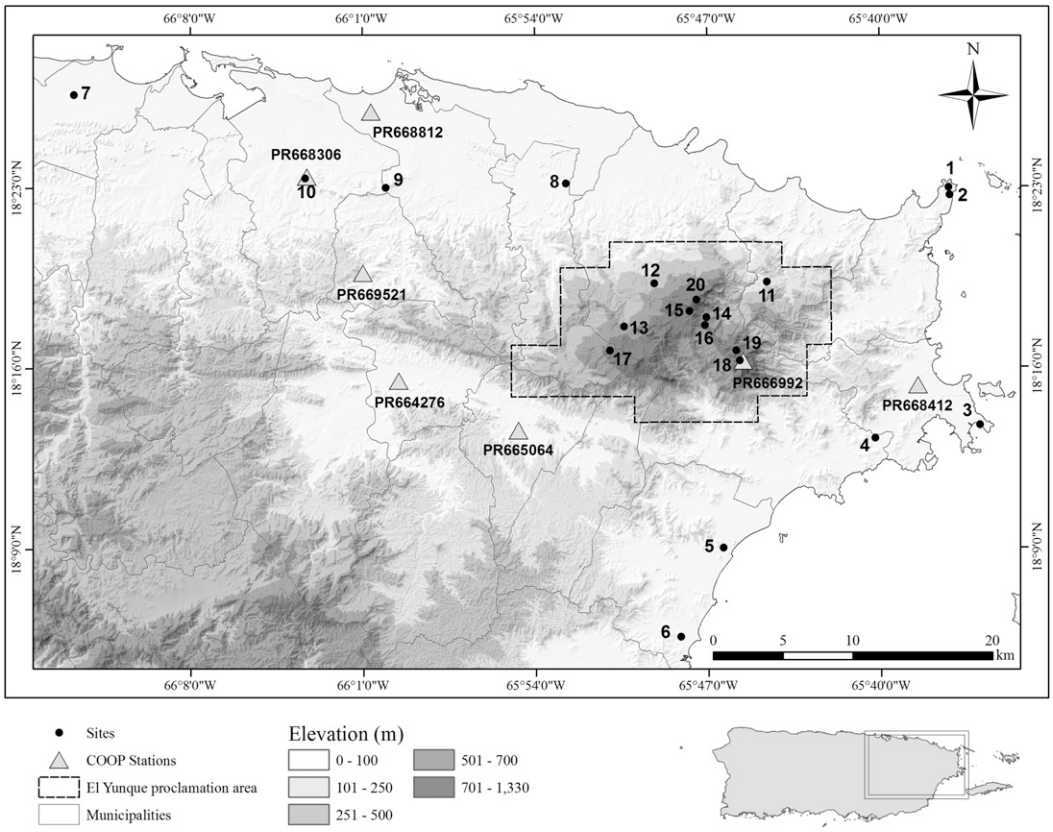

Figure 1. Site locations and COOP stations in northeastern PR. Also shown are the elevation contours, the El Yunque proclamation area, and the PR municipality boundaries.

pattern created by the easterly trade winds from the Atlantic Ocean (Larsen and Simon 1993). Interannual variability of rainfall is large due to broadscale storm patterns (Calvesbert 1970). In general, the Caribbean rainfall season is bimodal, with an early rainfall season (ERS; April–June) and a late rainfall season (LRS; August–November) (Briscoe 1966). In between (varying temporally by region) is the mild midsummer drought (Briscoe 1966; Comarazamy and González 2011; Curtis 2002). A longer and drier winter dry season (DS) occurs in December–March (Comarazamy and González 2011; García-Martinó et al. 1996; Giannini et al. 2000; Taylor et al. 2002). Temperature in PR is fairly constant temporally throughout the year (Calvesbert 1970). Interannual climate changes occur in the area from the El Niño–Southern Oscillation (ENSO) on a cycle of 3–5 years (Murphy and Stallard 2012), from the North Atlantic Oscillation (NAO; Taylor et al. 2002) and the sea surface temperature (SST; Jury and Gouirand 2011) on a decadal cycle, from the Atlantic multidecadal oscillation (AMO) on a cycle of 10–20 years (Hodson et al. 2010), and on a quasi-decadal scale from the interaction of all of these (Gouirand et al. 2012).

The main island is approximately 8900 km^2 with a thin strip of coastal plains, 8–16 km wide, surrounding steep igneous upland. Thus, orographic effects are a

major control on temperature and precipitation (Larsen and Simon 1993). Other mesoscale phenomena, such as sea breezes, mountaintop convection, and standing gravity waves, affect the local weather with frequent smaller storms (Carter and Elsner 1997). There are four mountain ranges within PR. One of these ranges, the Luquillo Mountains, dominates the geomorphology of the northeastern part of the island. At 10–20 km, these mountains rise from sea level to 1075 m, going from an average temperature of 25°C at the bottom to 18.5°C at the top (García-Martinó et al. 1996). Northeastern PR is the wettest region of the island with annual rainfall over 4500 mm (12 mm day^{-1}) in the upper elevations, compared to an islandwide average annual rainfall of 1778 mm (5 mm day^{-1}) (Calvesbert 1970). The vegetation in the upper reaches of the Luquillo Mountains is in a cloud forest and thus processes about 10% more water than annual rainfall resulting from the condensation of cloud droplets on plants (Weaver 1972). Most of the Luquillo Mountains are protected as part of the El Yunque proclamation area.

The 20 observation sites for this study were selected to be along an elevation gradient from sea level to the top of the Luquillo Mountains (see Figure 1), as well as to be spatially inclusive of the entire northeastern area and thus represent the different Holdridge life zones in northeastern PR (Ewel and Whitmore 1973; Holdridge et al. 1971). These are the subtropical dry, subtropical moist, subtropical wet, subtropical lower montane, subtropical lower montane rain, and subtropical rain forest life zones (Weaver and Gould 2013; Weaver and Murphy 1990).

3. Methods

In this study, precipitation and temperature were first observed at each of the 20 sites (Figure 1), and statistics were derived from the observed data. The derived statistics were compared with an outside data source to find biases in the collection method. Second, the derived statistics of the data were examined to determine the lengths the components of the periodic variation, since periodic variation must be accounted for in trend detection. Third, the derived statistics of the data were inspected to search for departures from the common statistical test assumptions: Gaussian distributed and independent. Finally, the derived statistics were analyzed for trends with robust methods, taking into account findings of the first three steps.

3.1. Data collection

The precipitation period of record (POR) was 12 years: August 2001–July 2013. There was one rain gauge located at each of the 20 sites. The gauge catches were observed and recorded at a varying frequency. Typically, each gauge was observed at the beginning of each month and one or two other times during each month. The mean daily precipitation (mm day^{-1}) then was determined between observations, resulting in 2–3 mean daily estimates per month. Site-specific mean observation intervals are listed in Table 1. See Medina et al. (2013) for more information about the gauge design.

Data were recorded as total precipitation since the last observation. From the raw data, daily total precipitation values were derived from the observation amount and the number of days between observations, where the days between observations are all given the same mean daily precipitation. If a gauge had a known operational

Table 1. Summary of quality of data collected at each site. Daily values (DVs) are derived mean daily in the case of precipitation and derived daily in case of temperature.

Elev (m)	Site ID	Site name	Precipitation DV % missing	Precipitation mean obs interval (days)	Precipitation DV from obs with interval ≥ 3 weeks	Temp DV % missing*	Temp 30-min obs % missing when DV exists	Temp DV % reaching censored level
0	1	Las Cabezas Dry	0.0	13.6	8.9	2.5	4.3%	22.3%
0	4	Las Cabezas Wet	0.7	13.6	8.5	6.7	6.1	23.6
0	6	Palmas del Mar	0.0	13.7	3.9	8.2	7.8	24.1
0	7	Humacao	0.0	13.1	7.7	4.6	4.4	25.2
2	5	Sabana Seca	0.0	14.1	8.4	6.9	6.7	20.9
7	2	Ceiba Dry North	0.0	13.8	5.7	5.6	5.2	18.8
23	9	Ford	0.0	13.8	7.0	9.8	9.4	12.2
26	3	Ceiba Dry South	0.0	14.0	7.6	4.5	4.2	7.6
81	10	Saint Just	1.6	13.9	5.9	13.4	12.8	20.7
100	8	Jardin Botánico	0.0	12.5	5.9	7.0	6.6	13.2
265	13	Sabana 4	0.0	13.4	6.1	4.1	3.7	9.8
434	11	El Verde	0.0	13.5	6.5	4.2	3.9	2.6
525	12	Rio Grande	0.0	13.6	6.0	5.8	5.5	0.1
634	14	UPR Nido	0.2	13.1	8.3%	6.0	5.6	3.9
751	15	Pico del Este Lower	0.0	13.3	9.7	9.4	12.6	0.5
811	16	El Toro	0.4	13.6	7.8	8.2	7.6	0.2
902	17	Mount Britton	0.1	13.3	9.1	6.4	6.5	3.0
953	18	Pico del Este Upper	0.0	13.3	10.1	8.7	8.1	0.2
954	19	Pico del Oeste	0.0	13.2	9.7	7.0	6.5	0.1
1000	20	El Yunque	0.0	13.2	8.3%	9.7	9.3%	0.9

* A daily value is considered missing if a quarter or more of the 30-min observations is missing sequentially in that day.

failure, the mean daily values were considered missing. Other researchers have noted that rainfall events are generally small (median daily rainfall of 3 mm) but numerous (267 rain days per year) (Schellekens et al. 1999). Thus, assuming every day contributes to the total rain observed during an observation interval is not an extreme assumption. Table 1 lists site-specific percent mean daily values missing and percent derived from an observation interval of 3 weeks or greater.

The temperature POR was 12 years, from September 2001 to August 2013. HOBO temperature loggers collected data at each site at 30-min intervals. Daily median, daily minimum, and daily maximum values were derived from the 30-min data. A daily value was considered missing if a quarter or more of the 30-min data were missing (sequentially) in that day. The percentage of missing 30-min

observations gave a measure of the accuracy of calculated daily temperature statistics (i.e., daily median, maximum, and minimum). See Table 1 for site-specific percentages of daily missing values and 30-min missing observations.

This study experienced a technical difficulty in that the temperature loggers became saturated above 38°C and temperatures greater than this were censored to 38°C. These censored observations thus affected calculation of the daily maximum temperature and the daily-mean temperature. The daily median temperature was not affected by the censoring since there was never a day in the POR where half of the 30-min observations are censored (nor is the daily minimum temperature affected). For this reason, the daily median was the preferred daily central tendency measure (CTM) over the daily mean for the study. See Table 1 for site-specific percentages of censoring.

Comparison with an outside data source

The data collected here were all collected with the same equipment by the same researchers. To assess any systematic error in the collection process, the data were compared to data from long-term National Weather Service (NWS) Cooperative Observer Program (COOP) stations. The COOP station data have been collected for different PORs, each by different researchers. Seven COOP stations are in the study area (see Figure 1 for locations). COOP stations report daily minimum temperature, maximum temperature, and precipitation.

To correlate the COOP station data with the site data collected in this study, the two datasets were transformed into equivalent formats. First, lapse rates were calculated with the COOP station data by fitting least squares regressions between the average daily minimum temperature, maximum temperature, and precipitation (averaged over each station's POR) and the elevations of the seven stations. Then the four COOP station datasets from locations close to sites from this study were adjusted to the elevation of the nearby site with the lapse rates. The precipitation data at these four COOP stations were recomputed to mean daily values averaged over the same observation interval as the nearby site. Overlapping time periods of data between the adjusted COOP station data and the nearby site data (non-censored) were then compared.

The results of the comparison are in Table 2. There was a high correlation coefficient between the adjusted COOP station data and the nearby site data for temperature: in all cases, $R \approx 0.99$. Precipitation had a much lower correlation coefficient: for all cases, $R \approx 0.32$, which was expected because of the localized nature of precipitation patterns. The best-fit ratio of the COOP station data to the nearby site data for the minimum temperature averaged to about one over the four cases, but the best-fit ratio for the maximum temperature averaged to about 0.9. It is suspected that the temperature loggers were affected by radiant heating, even though they were not located in the sun. Previous researchers have found that HOBO dataloggers sheltered under canopy where the canopy is in the sun can be subject to elevated temperatures, overestimating open-air temperatures (Hartz et al. 2006) and, furthermore, absorbing this extra heat to become miniature greenhouses (Dunham et al. 2005). If radiant heating was a problem, then the derived daily maximum temperatures would be biased, but derived daily minimum temperatures (occurring during the night) should be close to accurate.

Table 2. Comparison with outside data source.

COOP station ID	Elev of COOP station (m)	COOP temp and precipitation DV % missing	Nearby site ID	Nearby site elev (m)	Best-fit ratio: COOP*/site max temp DV $R \approx 0.99$	Best-fit ratio: COOP*/site min temp DV $R \approx 0.99$	Best-fit ratio: COOP*/site mean** precipitation DV $R \approx 0.32$
PR664276	49	2.4	—	—	—	—	—
PR665064	65	1.4	—	—	—	—	—
PR669521	35	6.1	—	—	—	—	—
PR666992	1051	77.0	18	953	0.87	0.97	1.00
PR668306	28	47.0	10	81	0.89	0.95	0.56
PR668412	10	39.9	3	26	0.91	1.09	0.60
PR668812	3	0.0	9	23	0.89	1.06	0.47

* COOP station data are adjusted to the elevation of the nearby site with the least squares lapse rate calculated from all seven COOP station POR means for daily minimum temperature, maximum temperature, and precipitation.

** COOP station data are averaged to the same interval as the site data.

COOP station PR666992 was the most similar to its nearby site in precipitation and minimum temperature data (see the best-fit ratios in Table 2). Using this station as a proxy, derived maximum temperatures from all sites were linearly adjusted by multiplying the values by a correction factor of 0.87 (the best-fit ratio for the maximum temperature for these COOP stations and nearby sites; see Table 2). A further reason for using the correction factor of 0.87 was that this is the smallest ratio found among the five comparisons and thus resulted in the largest adjustment giving the most generous error bar on the data.

The solid gray line in Figure 2 shows a CTM of a day of 30-min temperatures observations in the first 6 years (first half) of the POR. The CTM here is the mean over all 20 sites and all of the days in the first half of the POR. The solid black line shows the same CTM for the second 6 years (second half) of the POR. The calculated statistics of maximum, median, and minimum of the "CTM day" are marked in solid circles, and means are marked in solid squares. These CTM days were affected by censoring. There is no way of knowing the shapes of the noncensored CTM days but, with a studywide average of 10.5% of the days affected by censoring (see Table 1), assuming generously that every 30-min temperature that was observed at the saturation temperature was actually 5°C higher, the maximum temperatures of the two CTM days would be only 0.5°C larger than shown. So, an assumption was made here that the shapes of the noncensored CTM days would not be too different from that of the censored CTM days shown in Figure 2.

Satterlund et al. (1983) developed an equation for the temperature at every hour using only the maximum and minimum temperature and hours of rising temperature. Using the equation with the calculated minimum CTM day temperature and the linearly adjusted maximum CTM day temperature with correction factor of 0.87, an adjusted CTM day profile was computed. This is shown in the dashed gray and black lines in Figure 2, for the first and second half of the POR, respectively. The linearly adjusted maximum temperatures are shown as open circles; the minimum temperatures for the adjusted CTM days are necessarily the same as for the observed CTM days. With these adjusted CTM days, medians and means were

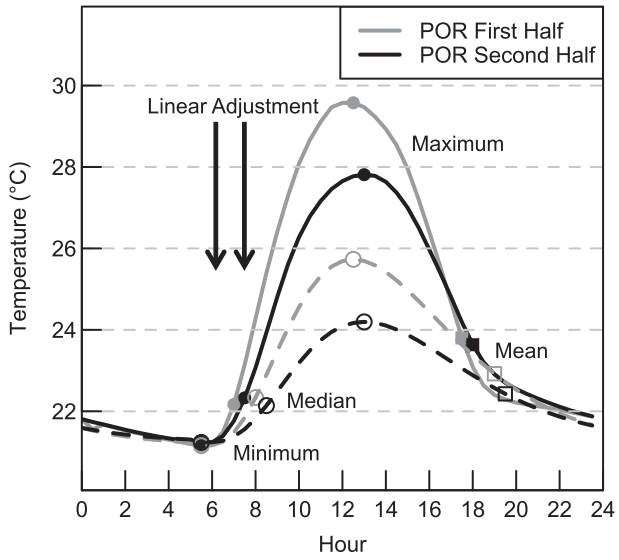

Figure 2. Solid lines show CTM of the mean of 30-min temperature observations over the first half and second half of days in POR, over all sites. Solid circles and squares show calculated statistics. Maximum daily temperatures are linearly adjusted by 0.87, and the dashed lines of adjusted CTM days are calculated with equation of Satterlund et al. (1983). Open circles and squares show calculated statistics from adjusted CTM days.

recalculated; they are shown in Figure 2 as open circles and open squares, respectively. The calculated adjusted CTM days medians were an average of 0.99 of the observed CTM days medians, and the calculated adjusted CTM days means were an average 0.95 of the observed CTM days means.

There is no way of computing a correction factor for the daily median temperature (or for the daily mean) since the COOP stations did not report daily median temperature (or mean), but the Satterlund et al. (1983) equation calculations shown in Figure 2 gave reason to believe that using the observed daily median temperatures without correction would not adversely affect any results. Additionally, Figure 2 gives support for using the daily median over the daily mean as a daily CTM in this study, since it shows that the daily median was less affected than the daily mean by overestimation of the daily maximum.

3.2. Determination of length of cycle and components of periodic variation

To use the most information available, it is desirable to look for trends using data from each periodic component in a cycle and account for this periodic variation, instead of simply taking yearly averages of data and throwing out the periodic components of the data (Shao and Li 2011). To perform the former, the length of a cycle and each periodic component must first be determined before attempting trend detection.

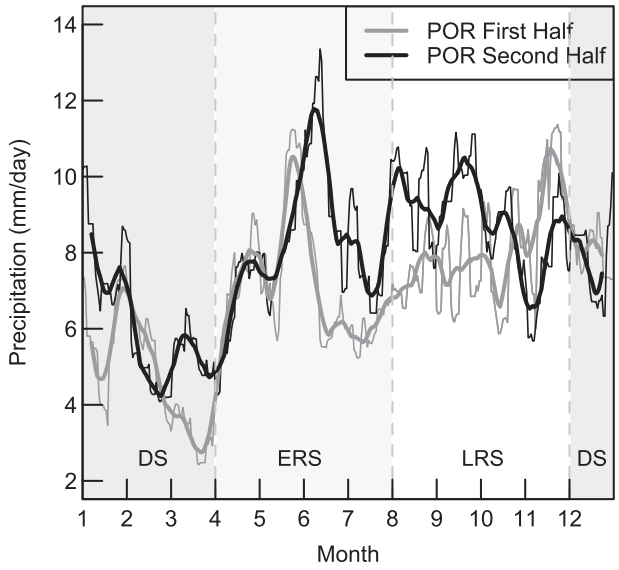

Figure 3. Solid thin lines show CTM of the mean of derived mean daily precipitation over the first half and second half of days in POR, over all sites. Solid thick lines show CTM smoothed with a 14-day moving average. Dashed lines and shaded regions delimitate 4-month terms of DS, ERS, and LRS.

It is commonly assumed in trend tests on climate variables that the dominant cycle or the length of the dominant periodicity is 1 year and the longest periodic component that can be expected to behave the same from cycle to cycle is 1 month (e.g., ElNesr et al. 2010; Partal and Kahya 2006). For example, this means that January climate from 1 year is comparable to January climate from another year but not to February climate from another year. However, the longest periodic component could hypothetically be longer or shorter than 1 month, and the dominant cycle could be longer or shorter than 1 year (Machiwal and Jha 2009; Serra et al. 2001; Valdez-Cepeda et al. 2012).

As discussed earlier, yearly precipitation in PR has a generally bimodal pattern, with a winter dry season, an early rainfall season, and a late rainfall season (Angeles et al. 2007; Briscoe 1966; Comarazamy and González 2011; García-Martinó et al. 1996; Giannini et al. 2000; Taylor et al. 2002). There is a brief midsummer drought between the ERS and LRS. The regional variability of the timing and magnitude of the midsummer drought, ERS, and LRS means that the bimodal pattern does not show up as a signal with the same frequency in every location (Briscoe 1966; García-Martinó et al. 1996; Zalamea and González 2008). Also, the effects of ENSO give interannual variability to the bimodal pattern even in the same region (Curtis 2002; Giannini et al. 2000). Thus, precipitation averaged over a region and a number of years will exhibit some smoothing of the yearly bimodal signal. The solid gray lines in Figure 3 show such a signal; these are the CTM of a year of the derived mean daily precipitation in the first 6 years (first half) of the POR. The CTM here is the mean over all 20 sites and all of the days in the first half of the POR. The thin line is the mean of the mean daily data, and the thick

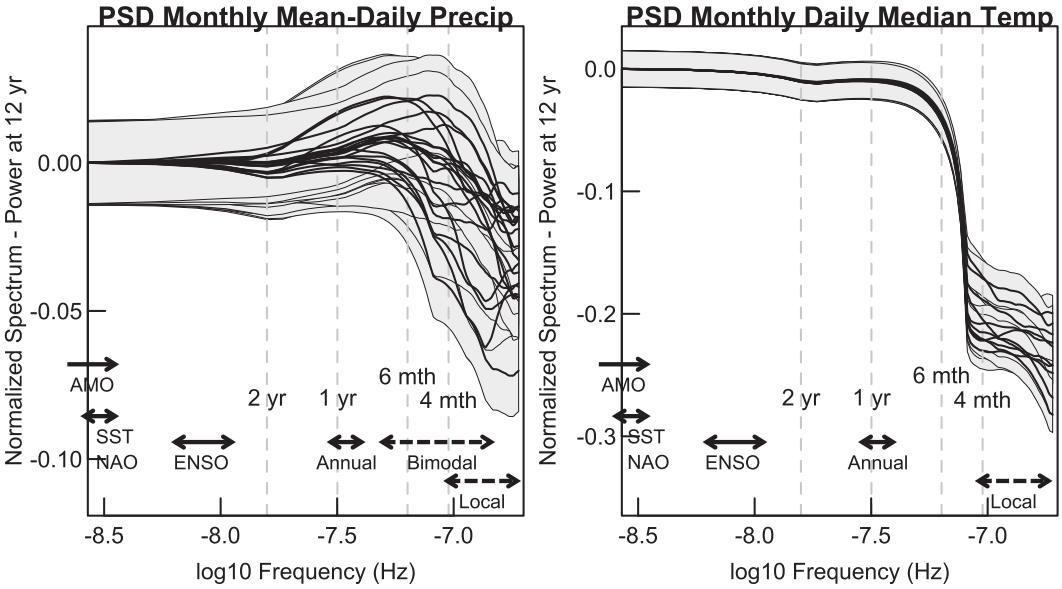

Figure 4. PSDs of monthly average mean daily precipitation and monthly average daily median temperature for each of the 20 sites (plotted on top of each other) for the entire POR. Shaded regions (with outlines) are estimated 90% confidence intervals. PSDs are normalized by subtracting the power at 12 years and dividing by maximum power. The frequency ranges of the large-scale influences (AMO, NAO, SST, and ENSO cycle) and the regional influences (annual cycle and bimodal precipitation cycle) are marked on the plots, as well as frequency range of local effects. The frequency range of the influences by the bimodal precipitation and local effects are less certain than the others, so they are denoted with a dashed line.

line is that mean smoothed with a 14-day moving average. The solid black lines show the same CTM for the second 6 years (second half) of the POR, with the thin line the mean daily data and the thick line the 14-day moving average. Roughly, the DS, ERS, and LRS can be broken into 4-month terms of December–March, April–July, and August–November, respectively, as shown in Figure 3.

Computing the power spectral density (PSD) of a time series is useful in determining the frequencies of the cyclic components of the data (Baldocchi et al. 2001; Gelpi and Norris 2005; Pelletier 2002; Richards et al. 2009; Wu et al. 2002). Here, the estimation of the PSD was done using the sine multitapers in which the number of tapers (and hence the resolution and uncertainty) vary according to spectral shape (Prieto et al. 2007; Riedel and Sidorenko 1995).

The PSDs of the monthly average mean daily precipitation and the monthly average daily median temperature for each of the 20 observation sites are shown in Figure 4 for the entire POR. The frequency ranges of the large-scale influences (AMO, NAO, SST, and ENSO cycles) and the regional influences (annual cycle and bimodal precipitation cycle) are marked on the plots, as well as frequency range of local effects. The PSDs for all 20 sites are plotted on top of each other; each PSD was normalized by subtracting the power at the 12-yr period and dividing

by the maximum power. The confidence intervals shown here are estimated in the simplest way possible from the number of degrees of freedom (two per taper) with 90% coverage (Prieto et al. 2007; Riedel and Sidorenko 1995). Precipitation data were averaged to each month so the signal is not affected by the observation interval since almost all observation intervals are shorter than a month. Temperature data were averaged to each month to ensure comparability between the plots. The PSDs of daily median temperature not averaged monthly but instead calculated with daily data do not look much different (not shown).

The PSDs showed agreement with previous research that PR has a periodic component to its precipitation that is less than 1 year. Each observation site had power at the 1-yr cycle but peaked in power at a period between less than 1 year and more than 4 months. In contrast, the PSDs for median temperature all peaked in power around 1 year and drop off in power at shorter periods (higher frequencies). The PSDs for daily maximum and daily minimum temperatures (not shown) looked very similar. Temperature was thus analyzed in the traditional way with a cycle of 1 year and 12 periodic components of 1 month. Precipitation was analyzed with a cycle of 1 year and 12 periodic components of 1 month but also with a cycle of 1 year and three periodic components of 4 months [the rainfall seasons of DS (December–March), ERS (April–July), and LRS (August–November)]. If the PSDs for precipitation had all showed a distinct 6-month peak in power, the precipitation could have been analyzed with a cycle of 6 months instead 1 year. Since the peaks are slightly different for each site, a cycle of 1 year and an alternative periodic component of 4 months representing the rainfall seasons of DS, ERS, and LRS were chosen for analysis.

Figure 5 shows an example at one site of the selecting the wettest month and the driest month of each rainfall season (DS, ERS, and LRS) to analyze for trends versus selecting a fixed generally wet month and generally dry month in each rainfall season. The black line in each plot shows the observed daily rainfall at site 20 over the entire POR. In the top plot, the observations that occurred in the driest month of each rainfall season are marked with light gray triangles and the observations that occurred in the wettest month of each rainfall season are marked with dark gray squares. Similarly, in the bottom plot, the observations that occurred in the generally driest month of each rainfall season (chosen from Figure 3 as March, July, and October) are marked with light gray triangles and observations that occurred in the generally wettest month of each rainfall season (chosen from Figure 3 as February, June, and September) are marked with dark gray squares. The high points of the data are marked much more often with the method used in the top plot (and likewise the low points) than in the method used in the bottom plot.

The rainfall seasons are known to shift spatially (from site to site) and temporally (from year to year) because of the effects of ENSO (Briscoe 1966; Curtis 2002; García-Martinó et al. 1996; Giannini et al. 2000; Zalamea and González 2008). This study aimed to calculate a measure of the trends of the drier and wetter months over the entire POR; thus, any method that assumed the rainfall seasons are the same spatially and temporally, such as the method illustrated in the bottom plot of Figure 5, was not desirable. Similarly, analyzing the trend in the driest months by only considering the designated DS (December–March)—or alternatively the trend in the wettest months by only considering the designated ERS and LRS—would suffer from the spatial and temporal variability of the rainfall seasons.

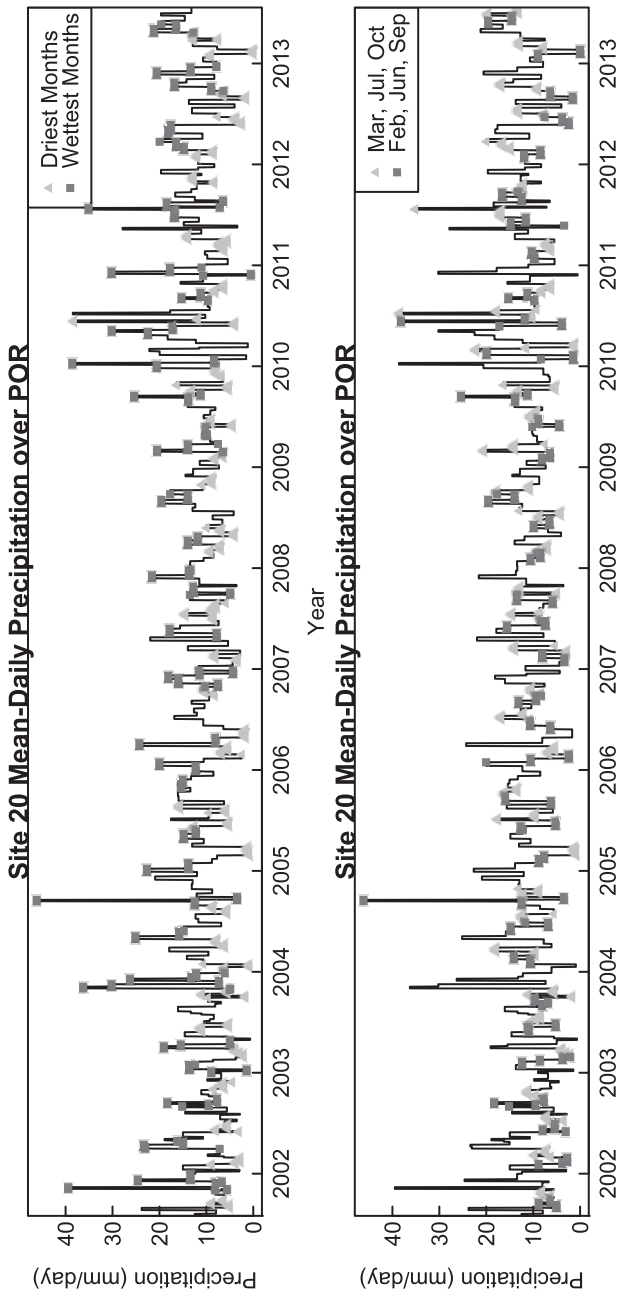

Figure 5. (top) For site 20, the observed daily rainfall is shown as a black line, with the observations that occurred in the driest month of each rainfall season (DS, ERS, LRS) marked with light gray triangles and the observations that occurred in the wettest month marked with dark gray squares. (bottom) The same data with the observations that occurred in the generally driest month of each season (chosen from Figure 3 as March, July, and October) marked with light gray triangles and the observations that occurred in the generally wettest month of each season (February, June, and September) marked with dark gray squares.

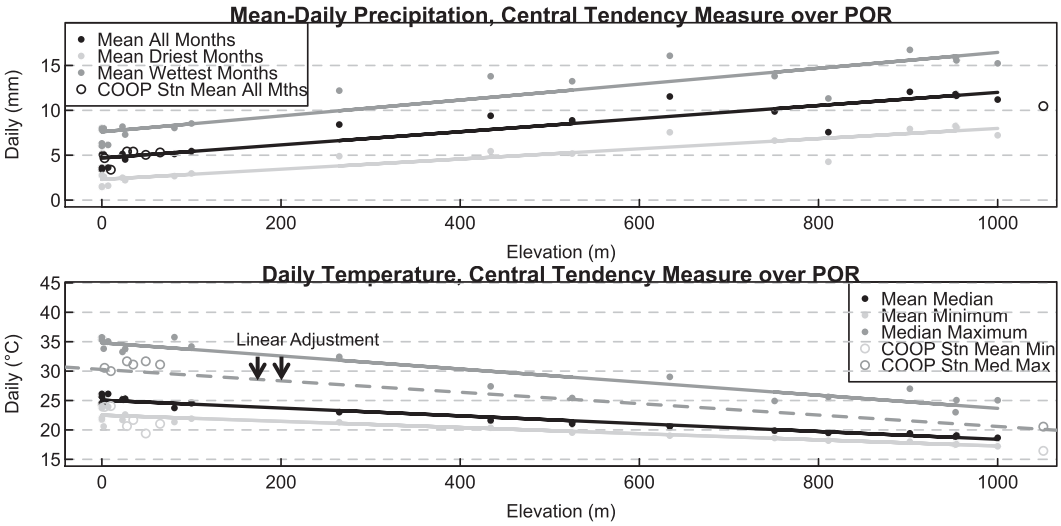

Figure 6. Solid circles are CTMs of mean daily precipitation and daily temperature at the observation sites, taken over the entire POR. Open circles are CTMs of COOP station data. Solid lines are linear least squares regressions to the site CTMs vs elevation. Dashed dark gray line is the solid gray line after linear adjustment by 0.87.

Therefore, in this study the maximum monthly precipitation in each 4-month periodic component (the rainfall seasons DS, ERS, and LRS) designated that month as a "wettest month" and the minimum monthly precipitation in each 4-month periodic component designated that month a "driest month." The wettest months and driest months were analyzed for trends over the POR; all of the months of data belonging to the 12 monthly periodic components were also analyzed for trends over the POR in the "all months" analysis. Each set of yearly realizations of the periodic components (12 months or 3 rainfall seasons) was analyzed for trends by separately by periodic component, and the results were summed into a single test statistic in an intrablock method of trend detection, discussed in more detail later.

A CTM of the all-months, driest-months, and wettest-months mean daily precipitation along the elevation gradient at each of the observation sites and the COOP stations (only for all months) is shown in Figure 6. This CTM is the mean over the entire POR. The solid lines are the linear least squares regressions to the site CTMs versus elevation (not the COOP station CTMs). Agreeing with previous studies, these regressions were highly significant, with p values much less than 0.001 (González and Luce 2013; Richardson et al. 2005).

In temperature, there is a cyclic signal shorter than 1 year, the daily diurnal heating and cooling signal. Methods of trend detection can only deal with one cycle and one shorter season, so this signal has to be removed from the data. To this end, the analysis here dealt with the derived daily median, minimum, and maximum temperatures and not the 30-min temperature observations directly. Again, all of the months of temperature data belonging to the 12 monthly periodic components were analyzed for trends over the POR. A CTM of the median, minimum, and maximum daily temperature along the elevation gradient at each of the observation

sites and the COOP stations (only for maximum and minimum) is shown in Figure 6. This CTM is the mean in the case of the median and minimum temperatures and the median in the case of the maximum temperatures over the entire POR. The median maximum is shown so as not have the CTM biased by the censoring (less than half of the maximum daily temperatures were derived from censored observations). The solid lines are the linear least squares regressions to the site CTMs versus elevation (not the COOP station CTMs). Again, these regressions were highly significant, with p values much less than 0.001. The dashed dark gray line shows the linear least squares regression line after multiplication by 0.87, the correction factor calculated from comparison to the COOP station data discussed previously. As expected, this line matches the COOP station daily maximum CTM values much better than the original linear least squares regression line.

3.3. Departures from common statistical test assumptions

For many common statistical trend tests, Gaussian and independent distributed data are assumed. If these assumptions are violated, alternative tests must be used. For data that are non-Gaussian, using a parametric trend detection method such as the t test and fitting a least squares trend line will exaggerate the significance of the trend (van Belle and Hughes 1984; Hirsch and Slack 1984; Machiwal and Jha 2009). However, if the data are indeed Gaussian and a nonparametric test is used, the nonparametric test has less power than the appropriate parametric test and thus it will be more likely that the test will not indicate a trend when in fact the generating process did have a trend. If data are assumed independent and are actually positively autocorrelated, there is an increased chance of a significant trend being detected when in actuality there is no trend (Bayazit and Önöz 2007; Cox and Stuart 1955; Hamed and Rao 1998; Hirsch and Slack 1984; Yue and Wang 2004; Yue et al. 2002; Zhang and Zwiers 2004). Conversely, assuming positive autocorrelation when the data are independent or negatively autocorrelated will result in increased chance of not detecting a true significant trend. Thus, it is very important to examine the distribution of the data and the independence or autocorrelation of the data before performing any trend tests.

3.3.1. Distribution of data

It has been long accepted that a Gaussian distribution does not best fit precipitation intensity, because of the improbability of negative events and the nonzero probability of infinitely large events (Buishand 1978; Katz 1977; Mielke 1973; Smith and Schreiber 1974; Todorovic and Woolhiser 1975; Woolhiser and Pegram 1979). The normalized PDFs of the three derived precipitation statistics for this study were estimated with the method of Silverman (1986) and are shown in black lines in Figure 7, for all 20 sites, along with the normalized Gaussian PDF in gray. The data at each site was normalized with a method robust to outlier influence; the median was subtracted and the result was divided by the median absolute deviation (MAD). The estimated PDFs do not look Gaussian.

The normalized estimated PDFs of the three derived temperature statistics are shown in black lines in Figure 8, for all 20 sites, again along with the normalized Gaussian PDF in gray (note the scale change on the plots). Again, the distributions

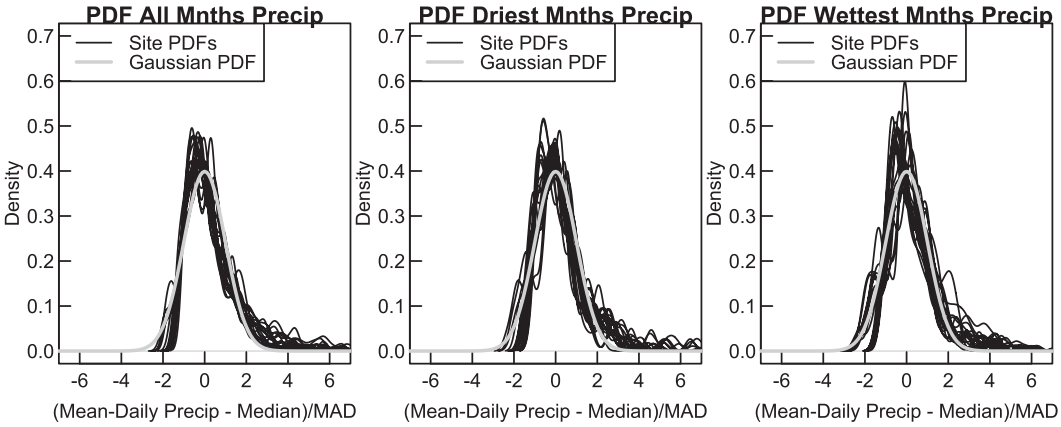

Figure 7. Black lines are estimated PDFs of normalized derived precipitation statistics (mean daily for all months, driest months, and wettest months) for each site, plotted on top of each other. The normalization is done for each site by subtracting the median and dividing by the MAD. The gray line is the normalized Gaussian PDF.

do not look Gaussian. Mean daily temperature has long been shown to have a Gaussian distribution (Thom 1952), but statistics of extreme temperature values (e.g., minimum, maximum) usually have a generalized extreme value distribution and are therefore non-Gaussian (Coles et al. 2001; Dixon 1950; Fisher and Tippett 1928; Gumbel 2012; Hughes et al. 2007; Jenkinson 1955; Smith 1989). Sample quantiles such as the median are also known to have non-Gaussian distributions (Kendall 1940; Noether 1948; Thompson 1936; Wilks 1948). Furthermore, censoring of the temperature observation would make distributions of the derived

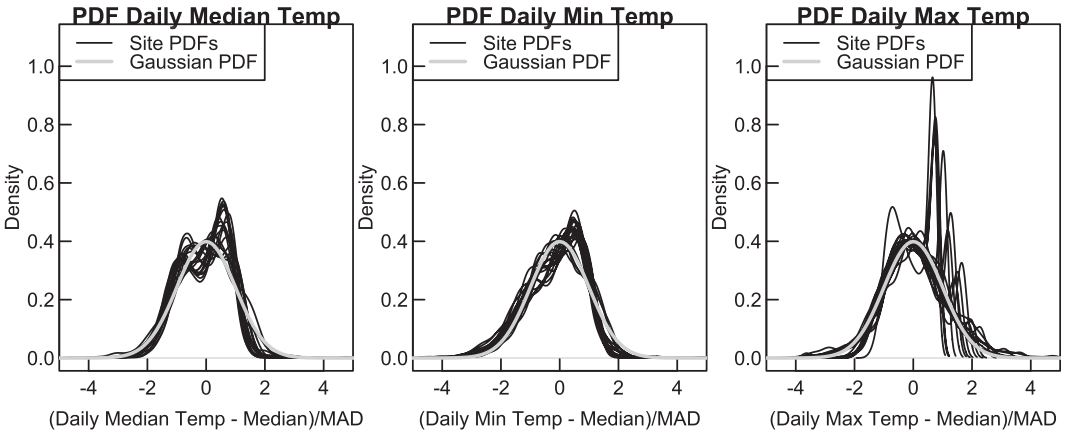

Figure 8. Black lines are estimated PDFs of normalized derived temperature statistics (daily median, minimum, and maximum) for each site, plotted on top of each other. The normalization is done for each site by subtracting the median and dividing by the MAD. The gray line is the normalized Gaussian PDF.

median and maximum non-Gaussian, even if the true median and maximum had a Gaussian distribution.

3.3.2. Independence or autocorrelation of data

The particularities of the data as discussed above means trend detections should be done with a nonparametric test that takes periodic variation into account and can handle censored and missing data. Thus, this study used the seasonal Mann–Kendall (SMK) test (Hirsch and Slack 1984; Hirsch et al. 1982). The advantages and disadvantages of the SMK test will be discussed in the next subsection. The test uses one observation (in this case, an ''observation'' of the derived statistic of precipitation or temperature) per periodic component (referred to by the SMK test as the ''season'') per cycle (in this case 1 year), and multiple observations in the same periodic component (in this case daily values) are averaged to make one periodic component observation. Again, in all temperature analysis and in the all-months precipitation analysis, a periodic component was 1 month. In the driest-months and wettest-months precipitation analyses, a periodic component was 4 months (the rainfall seasons of DS, ERS, and LRS) and the observation for the periodic component was the average mean daily precipitation from the driest or wettest of the 4 months, respectively.

Thus, the derived statistics only needed to be tested for independence in average values independent from one periodic component to the next periodic component. For each site, the Ljung–Box test was performed on the time series of average periodic-component-derived statistics of the precipitation and temperature data to test for autocorrelation at lag 1 (one unit is one periodic component). For details of the test, see Ljung and Box (1978). The data were said to be autocorrelated if the p value is less than 0.10. For all sites, all three of the average monthly (the periodic component)-derived statistics of temperature were found to be autocorrelated in the positive direction. For the average monthly (the periodic component)-derived statistics of precipitation analyzed for all months, some sites showed positive autocorrelation and some sites showed negative autocorrelation. For the average seasonally (the alternative periodic component)-derived statistics of precipitation analyzed for driest and wettest months almost all sites were found to be independent. This was to be expected since the data here might be 4 months apart in time.

3.4. Trend detection with periodic variation

The last step was to choose an appropriate method for detecting trends with periodic variation, taking into account the findings presented in the earlier subsections. The Mann–Kendall (MK) test is a intrablock ranking test that is powerful while being robust against missing, censored, and non-Gaussian data (van Belle and Hughes 1984; Kendall 1975; Mann 1945). It can be modified to deal with periodic and autocorrelated data in the form of the SMK test corrected for autocorrelation (Hirsch and Slack 1984; Hirsch et al. 1982). This study used the SMK test, and if a significant trend was detected, a version of the Sen's slope estimator (taking into account periodic variation) was used to calculate a linear trend (Hirsch et al. 1982; Sen 1968; Thiel 1950). Note that the Sen's slope estimator calculates a linear trend, thus assuming the detected trend is linear, but the SMK test finds only

if any monotonic trend is present, linear or not (Martínez et al. 2010; Serra et al. 2001; Tayanç and Toros 1997).

Let $X_{1g}, X_{2g}, \ldots, X_{ng}$ be a sequence of observations (the data) of n years ordered by time, for periodic component g (with p total periodic components). If there is more than one observation in a periodic component g and year i, then X_{ig} is the average of all observations (i.e., if the original observations are made daily, an observation of a month-long periodic component X_{ig} would be the average of the daily observations for that month). The periodic components are called "blocks" in SMK terminology. Then the SMK test is computed by calculating test statistics S_g on each block 1, 2, ..., p of data separately; the overall test statistic S combines the individual test statistics so that no cross-block comparisons are made,

$$S = \sum_{g=1}^{p} S_g \quad \text{where} \quad S_g = \sum_{k=1}^{n-1} \sum_{j=k+1}^{n} \operatorname{sgn}(X_{jg} - X_{kg})$$

$$\text{with} \quad \operatorname{sgn}(x) = \begin{cases} +1 & \text{if} \quad x > 0 \\ 0 & \text{if} \quad x = 0 \\ -1 & \text{if} \quad x < 0 \end{cases} \quad \text{and} \quad \operatorname{var}[S] = \sum_{g} \sigma_g^2 + \sum_{\substack{g,h \\ g \neq h}} \sigma_{gh}, \tag{1}$$

where $\sigma_g^2 = \operatorname{var}[S_g]$ and $\sigma_{gh} = \operatorname{cov}(S_g, S_h)$. The variance of S_g with tied and missing values is computed in Hirsch and Slack (1984). There is controversy on how to best use an MK test with autocorrelated data without stripping any potential trend (e.g., Bayazit and Önöz 2007; Hamed and Rao 1998; Yue and Wang 2004; Yue et al. 2002; Zhang and Zwiers 2004); here the variance of the test statistic is modified if autocorrelation exists following Hirsch and Slack (1984). Helsel and Frans (2006) extended the SMK test [Equation (1)] to the regional SMK (RSMK) test using sites as well as the periodic components as the blocking variable g. Periodic component fluctuations are not always constant over time so using intrablock methods instead of trying to remove the periodic variation with functional adjustment is the preferred technique here (Zhang and Qi 2005). Sen's slope estimator Q modified for periodic variation is the median of all pairs in all periodic components,

$$Q = \operatorname{median}\left(\left[\left[\left[\frac{X_{jg} - X_{kg}}{j - k} \right]_{k=1}^{k=n-1} \right]_{j=k+1}^{j=n} \right]_{g=1}^{g=p} \right). \tag{2}$$

The SMK test was performed for each site and the RSMK test was performed for northeastern PR as a whole, all for each of the six derived statistics (mean daily for all-months, driest-months, and wettest-months precipitation and daily median, minimum, and maximum temperature). So, if the p value was less than or equal to a set level α, the trend was considered significant. As described earlier, the daily maximum temperature (but not daily minimum or median temperature to a large extent) suffered from being derived from censored 30-min temperatures and also from potential radiant heating of the sensors possibly linearly inflating the derived values (see Tables 1 and 2 and Figure 2). The SMK and RSMK tests are robust to the censoring at the same level, and any monotonic increase in the data will not affect the ranking in Equation (1), so the tests of possible trend were resistant to these problems.

However, Sen's slope estimator in Equation (2) was affected by these problems. Sen's slope must therefore be reported as a range for the daily maximum temperatures. Sen's slope was estimated using the daily maximum temperatures from the observed 30-min temperatures, from the observed 30-min temperatures with the censored values increased to the maximum possible true value (100°C), and from the observed 30-min temperatures linearly adjusted by the correction factor 0.87 (from Table 2).

A larger p value cutoff of $\alpha = 0.10$ was chosen for this entire study over the more traditional 0.01 or 0.05 because many of the climate trend studies covering PR (Burrowes et al. 2004; Greenland and Kittel 2002; Heartsill-Scalley et al. 2007; Stephenson et al. 2014; Torres-Valcárcel et al. 2014; Vose et al. 2005) have used a t test and fit a least squares trend line, which exaggerates the significance of the trend, reporting a reduced p value, for non-Gaussian datasets.

4. Results

Results for the SMK tests with significant two-sided trend analyses at the $\alpha = 0.10$ level are given in Table 3, and results for the RSMK tests are given in Table 4.

4.1. Regional and elevation gradient patterns of precipitation trends

In the derived precipitation statistics, the RSMK test at the $\alpha = 0.10$ level found significant regional trends for mean daily months and driest months (of the rainfall seasons of DS, ERS, and LRS) (see Table 4). The RSMK test did not find a significant regional trend for mean daily wettest months. This was expected since the SMK test only found one site with a significant trend (see Table 3). The data were positively autocorrelated between blocks in the regional compilation of each of the three derived precipitation statistics. For mean daily all-months and driest-months precipitation, Sen's slopes were estimated at each site and are shown plotted against site elevation in Figure 9. No plot was made of Sen's slopes against elevation for mean daily wettest-months precipitation. Sen's slopes from sites with significant trends detected by the SMK test at the $\alpha = 0.10$ level are shown in solid circles in Figure 9; sites with insignificant (but contributing to the significant regional trend) trends are shown in open circles. A linear least squares regression line was fit to only the Sen's slopes at sites with significant trends and is shown in Figure 9.

The Sen's slope (the linear trend) estimated for the whole region mean daily all-months precipitation was slightly more positive than that of the whole region mean daily driest-months precipitation (see Table 4). The p value after adjustment for autocorrelation for both was less than 0.10. The linear least squares regression of the sites with significant trends results for all-months precipitation had a positive slope of the linear trends with elevation that was not particularly significant (p value = 0.139) (see Table 4 and the top plot of Figure 9). However, for driest-months precipitation, the linear least squares regression of the sites with significant trends results had a 3 times larger slope of the linear trends with elevation that was highly significant (p value = 0.001) (see Table 4 and the bottom plot of Figure 9).

Table 3. Sen's slopes for sites with significant trends detected at the $\alpha = 0.10$ level.

Elev (m)	Site ID	Sen's slope change in mean daily all-months P (mm day^{-1} yr^{-1})	Sen's slope change in mean daily driest-months P (mm day^{-1} yr^{-1})	Sen's slope change in mean daily wettest-months P (mm day^{-1} yr^{-1})	Sen's slope change in daily median T (°C yr^{-1})	Sen's slope change in daily min T (°C yr^{-1})	Sen's slope change in daily max T (°C yr^{-1})*
0	1	—	—	—	—	—	−0.29 (−0.22) −0.19
0	4	—	—	—	—	—	−0.32 (−0.26) −0.23
0	6	0.11	—	—	0.09	0.12	−0.56 (−0.40) −0.35
0	7	—	—	—	0.07	—	−0.82 (−0.51) −0.44
2	5	—	0.04	0.25	0.07	0.12	−0.56 (−0.50) −0.43
7	2	—	—	—	—	—	—
23	9	0.16	—	—	—	—	−0.21 (−0.21) −0.19
26	3	—	—	—	—	—	—
81	10	0.09	0.08	—	−0.04	—	−0.46 (−0.31) −0.27
100	8	—	—	—	—	—	−0.41 (−0.41) −0.35
265	13	0.20	0.20	—	−0.05	—	—
434	11	0.32	0.26	—	0.04	0.04	−0.19 (−0.19) −0.16
525	12	—	0.18	—	—	—	—
634	14	0.21	0.26	—	—	—	—
751	15	0.23	0.28	—	—	—	−0.15 (−0.15) −0.13
811	16	0.12	—	—	0.07	0.05	—
902	17	0.23	0.27	—	—	—	−0.58 (−0.58) −0.50
953	18	0.20	0.23	—	—	—	−0.17 (−0.17) −0.15
954	19	0.19	0.25	—	—	—	−0.27 (−0.27) −0.24
1000	20	0.25	0.37	—	—	—	−0.25 (−0.25) −0.22

* Low end of range is from using censored values increased to maximum–maximum temperature, middle of range from using data as is, and high end of range from using data linearly adjusted to agree with COOP station temperatures.

Table 4. Regionwide Sen's slopes.

Method	Sen's slope change in mean daily all-months P (mm day^{-1} yr^{-1})	Sen's slope change in mean daily driest-months P (mm day^{-1} yr^{-1})	Sen's slope change in mean daily wettest-months P (mm day^{-1} yr^{-1})	Sen's slope change in daily median T (°C yr^{-1})	Sen's slope change in daily min T (°C yr^{-1})	Sen's slope change in daily max T (°C yr^{-1})[a]
RSMK on all sites	0.11	0.09	—	—	0.02[b]	−0.26 (−0.24) −0.21
Sites with significant SMK tests[c]	$0.000\,076x + 0.15$[b]	$0.000\,215x + 0.09$	—	—	0.08	−0.37 (−0.32) −0.27

[a] Low end of range from using censored values increased to maximum–maximum temperature, middle of range from using data as is, and high end of range from using data linearly adjusted to agree with COOP station temperatures.

[b] These numbers have a higher p value than the $\alpha = 0.10$ level. See text for more details.

[c] Linear least squares regression is fit to Sen's slopes with significant SMK test results, if the regression line has only a significant intercept then the mean of the Sen's slopes is reported; otherwise, the regression line equation is reported with variable x as the elevation of the site in meters.

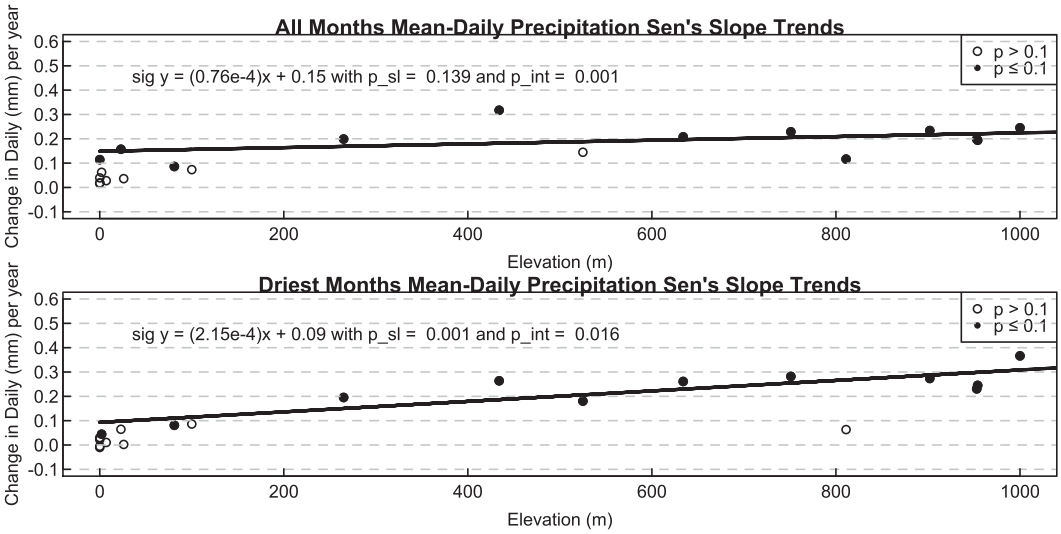

Figure 9. Circles are estimated Sen's slopes, or linear trends, of derived precipitation statistics at the observation site elevations (mean daily for all months and driest months). Solid circles indicate a *p* value ≤ 0.10 for the SMK test at that site; open circles indicate the opposite. In each plot, solid circles (called sig(nificant) y) are used to compute the linear least squares regression line of trend vs elevation, with its details annotated in the plot. The *p* values of the slopes are "p_sl" and the *p* values of the intercepts are "p_int."

Precipitation change is often reported as percent. Using the linear least squares regressions of the site CTMs versus elevation in Figure 6 ($y = 0.005\,67x + 1.93$ and $y = 0.007\,85x + 3.48$ for all months and the driest months, respectively) and the linear least squares regressions of the Sen's slopes versus elevation in Figure 9, an average percent change per year was computed. The result was $+4\%\ \mathrm{yr}^{-1}$ at sea level decreasing to $+2\%\ \mathrm{yr}^{-1}$ at 1000 m for all months and $+5\%\ \mathrm{yr}^{-1}$ at sea level decreasing to $+4\%\ \mathrm{yr}^{-1}$ at 1000 m for the driest months.

4.2. Regional and elevation gradient patterns of temperature trends

In all three derived temperature statistics, multiple sites showed significant trends with the SMK test at the $\alpha = 0.10$ level, but the RSMK test only found significant regional trends at the $\alpha = 0.10$ level for daily maximum temperature (p value of the daily minimum regional trend was not quite small enough) (see Table 4). The data were positively autocorrelated between blocks in the regional compilation of each of the three derived temperature statistics. For daily median, minimum, and maximum temperature, Sen's slopes were estimated at each site and are shown plotted against site elevation in Figure 10. Sen's slopes from sites with significant trends detected by the SMK test at the $\alpha = 0.10$ level are shown in solid circles in Figure 10; sites with insignificant (but contributing to the significant regional trend) trends are shown in open circles. A linear least squares regression

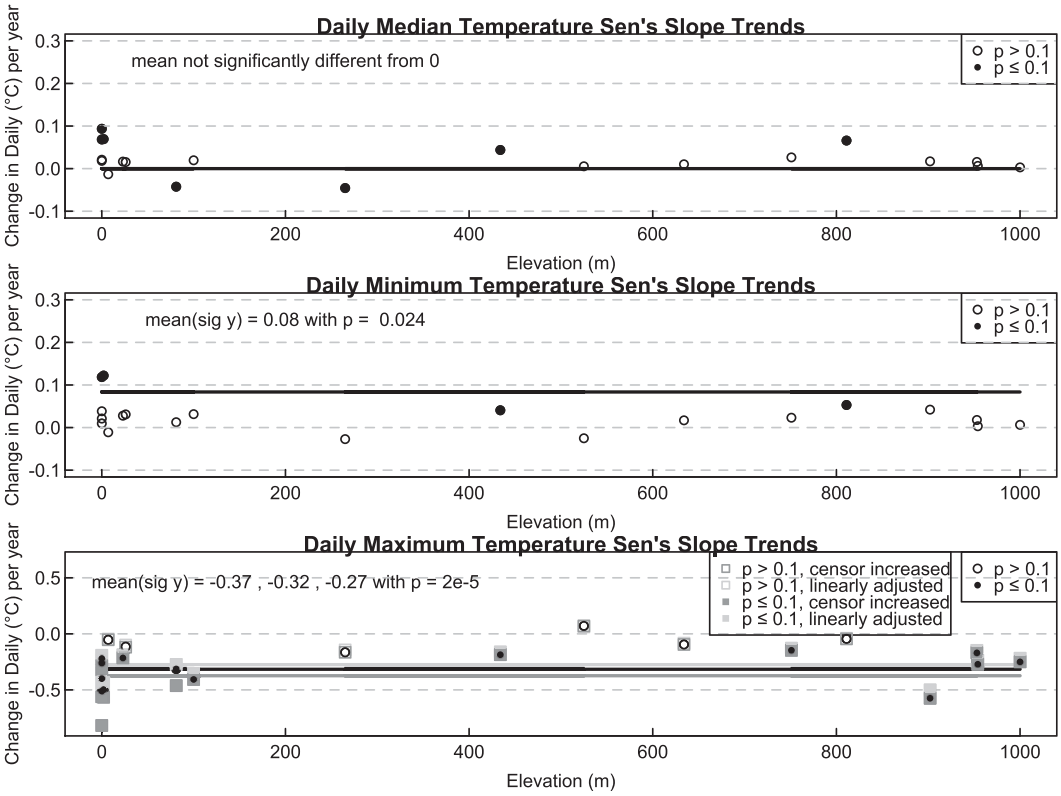

Figure 10. Circles are estimated Sen's slopes or linear trends of derived temperature statistics at the observation site elevations (daily median, minimum, and maximum). Solid circles indicate a *p* value ≤ 0.10 for the SMK test at that site; open circles indicate the opposite. In each plot, solid circles (called sig(nificant) *y*), are used to compute the linear least squares regression line of trend vs elevation, with its details annotated in the plot. The *p* values of the intercepts are annotated. None of the derived statistics have significant slopes to their regression lines. Daily maximum temperature has three estimates (from observations in black, from observations with censored values increased to the maximum possible value of 100°C in dark gray, and from observations linearly adjusted by 0.87 in light gray).

line was fit to only the Sen's slopes at sites with significant trends. None of the derived temperature statistics had even a slightly significant relationship between linear trend and elevation (i.e., the regression line did not have a significant slope), but the intercept of the regression line was significant for daily minimum and maximum so the mean of the significant trends is reported for these (see Table 4) and a horizontal line is plotted at the mean of the significant trends in Figure 10. The mean of the significant trends in the daily median was not significantly different from zero.

There was no significant trend found for the whole region daily median temperature. There were seven sites with significant trends from the SMK test (see

Table 3), but they were not in the same direction so it was expected that the regional test would not find a significant trend. All Sen's slope linear trends are shown in the top plot of Figure 10.

There was slight evidence that the trend for the whole region daily minimum temperature was small and positive (see Table 4) since the p value after adjustment for autocorrelation was 0.12 (slightly above the $\alpha = 0.10$ level). In contrast, there was strong evidence that the trend for the whole region daily maximum temperature was a magnitude larger in size and in the opposite direction, negative, since the p value for the RSMK test was 0.02. In the bottom plot of Figure 10, the range of Sen's slopes at each site is plotted, with the slopes (and line of mean of significant slopes) from the data derived from the observed 30-min temperatures in black. The lower bounds on the slopes from the data derived from the observed 30-min temperatures with the censored values increased to the maximum possible true value (100°C) are in dark gray. The upper bounds on the slopes from the data derived from the observed 30-min temperatures linearly adjusted by the correction factor 0.87 are in light gray. Note that the points plotted on top of each other in the bottom plot of Figure 10 were either all significant or all not significant, since the results of the SMK test do not change from the two adjustments to the data.

5. Discussion

This section discusses the trend results found here, the trend results found elsewhere and how these two sets of results can be reconciled in regards to the future of northeastern PR.

5.1. Trends found in this study

The results showed a positive trend from 2001 to 2013 in daily-mean precipitation in northeastern PR considering all months of the year with a slightly larger positive trend in driest-months daily-mean precipitation. The trends were around $+0.1\,\mathrm{mm\,day^{-1}\,yr^{-1}}$. The driest months were the driest months in each of the dry season, early rainfall season, and late rainfall season. Analyzing the driest months of the DS, ERS, and LRS (as opposed to the rainfall seasons as a whole) allowed a pattern to be seen even though the rainfall seasons exhibit spatial and temporal variability (Briscoe 1966; Curtis 2002; García-Martinó et al. 1996; Giannini et al. 2000; Zalamea and González 2008). There was evidence that the magnitude of the trend in the driest-months precipitation was linearly increasing as elevation increases; the evidence for the linearly increasing trend with elevation was much stronger for driest months than when considering all months of the year (see Figure 9). Since the mean yearly amount of precipitation was greater at higher elevations (see Figure 6), this means the wetter higher elevations got wetter from 2001 to 2013 and the drier lower elevations got slightly wetter. When the increase was calculated as a percent, the result at the average elevation of 500 m was $+3\%\,\mathrm{yr^{-1}}$ for all months and $+4.5\%$ for the driest months, with a smaller percentage increase at the higher elevations and a larger percentage increase at the lower elevations. Since the wetter months of the rainfall seasons did not show any trend, there was a trend of a shrinking difference between the drier months and the wetter months and more so at higher elevations.

For temperature, the results showed no trend in daily median temperature from 2001 to 2013 but a positive trend in the daily minimum temperature (+0.02°C across the region) and a larger negative trend in the daily maximum temperature (likely an order of magnitude larger in size). Thus, the results showed a trend of decreasing diurnal temperature range (DTR). There was more evidence that the negative trend in daily maximum temperature was regionwide than was the positive trend in daily minimum temperature. The trends in temperature appeared to be uniform across the elevation gradient (see Figure 10). The direction of the daily maximum trend was reliably computed (negative), but the size of the trend was less certain because of instrument errors of radiant heating (creates observations that need to be adjusted) and saturation (creates censored observations).

Using outside data sources and assuming a linear adjustment was satisfactory, the observations were scaled and an estimation of the trend magnitude was computed. If the effect of the radiant heating of the sensors was nonlinear such that the hottest temperatures were elevated proportionally more than the average hot temperatures, then the estimated size of the negative trend should have been less. Conversely, if the effect of radiant heating was a scalar overestimation and not a linear effect, the trend of the actual maximum temperatures should have been the same as that estimated with the observed data.

Data from censored observations were all raised to a maximum possible value of 100°C to compute a bound on trend magnitude. The trend was thus estimated to not be any more negative than $-0.26°C\,yr^{-1}$ across the region. If the maximum possible value was lowered to a more likely (but not inconceivable to exceed) 45°C, the bound would still be computed at $-0.26°C\,yr^{-1}$.

5.2. Trends from previous research on other time periods

Previous research has been done on trends in precipitation and temperature on past time periods and (projected) future time periods. The past trends are from data at the scale of a few sites in northeastern PR, and the future trends are from global climate model data at the scale of the whole Caribbean. Because the past and future trend studies use such small and large scales, respectively, they are not able to detect differences in trends along an elevation gradient.

5.2.1. Past climate trends

Generally, increasing trends have been found in past climate precipitation, in agreement with the results found in this study. Greenland and Kittel (2002) analyzed one of the longer temporal precipitation records in northeastern PR, resulting in estimates of the trends from 1932 to 1994 at one site. They report a significant increasing trend for precipitation in the DS only (recalculated to mean daily of $+0.032\,mm\,day^{-1}$). In contrast, Torres-Valcárcel et al. (2014) found mostly decreasing trends in precipitation at 139 stations across PR for 30-yr periods for 1900–90. However, although the study does not separate out results by geographic region such as the northeast, they do show pictorially that the wet forest (most of northeastern PR is wet forest) has a possible increasing trend in the 30-yr periods, and the decreasing trends are coming from the moist and dry forests. Furthermore,

they found increasing trends at across PR in the recent period of 1990–2007. Beck et al. (2013) also found an increasing trend of 0% yr^{-1} to +0.1% yr^{-1} from the seven COOP stations (see Figure 1) in northeastern PR for 1955–2010. They did not report the site-specific trends, making no inferences about elevation gradient trend patterns. They also did not report significance levels. However, Méndez-Lázaro et al. (2014) did report that these increasing trends were significant at two of the COOP stations and one other site for 1955–2009 (they only looked at three of the COOP stations). Using more recent past data, Durre et al. (2009) inferred an increasing precipitation trend from 1973 to 2006 since they found an increasing trend in precipitable water in the atmosphere at a site in PR (and the whole of the eastern United States). Scholl and Murphy (2014) studied shorter-term trends from 1992 to 2012 at two sites and years 2000–11 at one site and found about +0.4 mm day^{-1} yr^{-1} for all three sites. One previous study did find a decreasing trend for precipitation from 1988 to 2003 of −0.20 mm day^{-1} yr^{-1} at one site in northeastern PR (Heartsill-Scalley et al. 2007).

Previous research in past climate temperature seems to indicate that longer-term trend is predominately an increasing maximum daily temperature, while the shorter-term trend is predominately a decreasing DTR from the increasing minimum daily temperature. Greenland and Kittel (2002) found longer-term trends for temperature (1932–94) at one station with a mean daily trend of +0.007°C yr^{-1}, a minimum daily trend of −0.009°C yr^{-1}, and a maximum daily trend of +0.024°C yr^{-1}. Conversely, Burrowes et al. (2004) found an increasing trend for minimum daily temperature at one station of +0.02°C yr^{-1}, in agreement with the results here. Their study was shorter term (although longer than and before this study), covering the years 1970–2000. Stephenson et al. (2014) saw a continuance of this trend at one station in PR, with an increase of +0.03°C yr^{-1} for minimum daily temperature for the years 1986–2010. Their study also agreed with the direction of the maximum daily temperature trend found here but not with the magnitude; they found a decrease of −0.01°C yr^{-1} for maximum daily temperature for the years 1986–2010. Notably, their results showed that most of the surrounding Caribbean countries had both increasing trends in minimum and maximum daily temperature (still with a decreasing trend in DTR) and the decreasing trend in maximum daily temperature in PR is more of local effect (Stephenson et al. 2014). Vose et al. (2005) also found regional-averaged increasing trends in minimum daily temperature and maximum daily temperature and a decreasing trend in DTR for the years 1979–2004, with smaller-magnitude trends for the years 1950–2004.

5.2.2. Future climate trends

Studies of future climate scenarios from global climate models (GCMs) covering PR agree on their prediction of an increasing trend for temperature of 0.01°C yr^{-1} to +0.03°C yr^{-1} (+1° to +3°C in 100 years), but the direction and timing of the precipitation trend is more uncertain ranging from −0.5% yr^{-1} (−50% in 100 years) to +0.2% yr^{-1} (+10% in 50 years) and how the specific rainfall seasons will change from short term to long term is also controversial (Angeles et al. 2007; Campbell et al. 2011; Hall et al. 2013; Karmalkar et al. 2013).

Regional climate models (RCMs) that allow SSTs to dynamically interact with changes in the atmosphere (models not yet developed) may give different results than the steady drying simulated by most GCMs (Karmalkar et al. 2013). GCMs simulate large-scale convective processes and do not simulate the orographic processes on small mountain ranges such as the Luquillo Mountains, nor can they resolve the timing of climate change effects on localized areas (Scholl and Murphy 2014). This may be why the results of this study are not in agreement with future climate predictions.

5.3. Physical mechanisms behind trends

The differences in the trends along the elevation gradient have not been studied previously in PR, but they have been studied in other areas. Observational and theoretical studies have suggested that higher elevations can identify interannual climatic fluctuations and longer-term climate change more readily than lower elevations, because the greenhouse gas warming signal is more clearly detected at the higher elevations (Beniston and Rebetez 1996; Giorgi et al. 1997; Li et al. 2012; Liu et al. 2009). Some studies have found evidence for a stabilizing atmosphere causing differences in the trends along the elevation gradient (Cao et al. 2007; Giambelluca et al. 2008). Their results show an enhanced increasing trend in temperature with elevation (but would be also supported by a diminishing decreasing trend in temperature with elevation). The inability of this study to detect a difference in the temperature trends along the elevation gradient may be due to the short record of data, as suggested by Liu et al. (2009).

The 12 years of data analyzed here is not long enough to separate true climate change from the decadal cycle of the NAO (Taylor et al. 2002) and SST (Jury and Gouirand 2011), the 10–20-yr cycle of the AMO (Hodson et al. 2010), or the quasi-decadal cycle of the interaction of all these cycles (Gouirand et al. 2012). It is potentially long enough to rule out causality by the ENSO 3–5-yr cycle (Murphy and Stallard 2012). Stephenson et al. (2014) show evidence that the positive phase (and transitional phase) of the AMO starting in the late 1980s is the driver for increasing precipitation and higher temperatures in the Caribbean. Continued monitoring will be necessary to assess climate changes.

Nonclimatic changes may also be responsible for the trends found here. A study by Torres-Valcárcel et al. (2014) suggests that, if the positive trend in precipitation is not simply part of a climate cycle, it may be due to increasing urban development and a higher sensitivity or response to urban impacts in wetter areas of PR such as the northeast. Giambelluca et al. (2008) found evidence in Hawaii that urbanization has countered daytime warming and enhanced nighttime warming, possibly resulting from cloud cover increase at night. The results from this study support such a hypothesis; a decreasing trend in maximum temperature (occurring during the day) and an increasing trend in minimum temperature (occurring during the night) were found in northeastern PR. Future studies in northeastern PR will focus on cloud base height measurements and the analyses of the relationship of cloudiness and changes in climate (precipitation, temperature, and radiation) along the elevation gradient.

5.4. Implications

The objective of this study was to look at the difference in the trends in statistical components of precipitation and temperature along an elevation gradient, something that had not previously been done in PR. Cloud forest ecosystems only occur at the highest elevations in northeastern PR and are very sensitive to changes in central measures (e.g., mean, median) of precipitation and temperature and also to changes in statistical components of precipitation and temperature (e.g., driest months, daily maximum) (Foster 2001; Still et al. 1999). Amphibians that now only exist below 400 m are very sensitive to changes in daily minimum temperature and drought (Burrowes et al. 2004). Forest types are distributed by elevation and changes to the pattern of precipitation and temperature along the elevation gradient would change the distribution, which could potentially affect the allocation of endemic species (Scatena 1998). The effect of nighttime warming (increase in minimum temperature) in enhancing nighttime respiration has been shown to favor some plant species over other species, reducing diversity in ecosystems (Alward et al. 1999). These and many other examples are the reason that patterns of trends along the elevation gradient and not just the overall trends are important. It is significant that this study found a difference in the trends in statistical components of precipitation along an elevation gradient. Tropical ecosystems across the globe are highly sensitive to climate, and individual regions are able to support their diversity of species because of their variability of climate across elevation gradients (Denslow 1987; Enquist 2002; Halpin 1997; Hilbert et al. 2001; Phillips and Gentry 1994; Vitousek 1998). The results from this study emphasize that differing patterns of climate change across the elevation gradients of tropical ecosystems should be considered a possibility when looking toward the future.

6. Conclusions

The results of this study show that components of precipitation had different absolute and percentage trends along an elevation gradient in northeastern PR from 2001 to 2013. The driest months of the rainfall seasons had a positive trend that increased as elevation increased, and the overall positive precipitation trend may have also increased in magnitude with elevation. In temperature, the trends did not appear different along the elevation gradient, but it is notable that the range of the daily temperature changed without necessarily changing the daily median temperature, by a decreasing daily maximum temperature trend. Studies of precipitation and temperature trends in PR and tropical regions across the globe should look at how the trends in the different components change with elevation, since the diversity of tropical biological life is highly elevation dependent and different species are sensitive to different components of precipitation and temperature.

Acknowledgments. This research was supported by Grants DEB 0080538, DEB 0218039, and DEB 0620910 from U.S. National Science Foundation to the Institute for Tropical Ecosystem Studies, University of Puerto Rico, and to the International Institute of Tropical Forestry (IITF) USDA Forest Service, as part of the Luquillo Long-Term Ecological Research Program. The U.S. Forest Service (Department of Agriculture) Research Unit, the Luquillo Critical Zone Observatory (EAR-1331841), and the University of Puerto

Rico gave additional support. We thank Maya Quinoñes at the USDA Forest Service International Institute for Tropical Forestry for help with Figure 1. Field assistance was provided by Humberto Robles, Samuel Moya, Carlos Estrada, and Carlos Torrens. William A. Gould, D. Jean Lodge, and Ariel E. Lugo graciously provided comments on an earlier version of the manuscript. We also would like to thank our anonymous reviewers. Any use of trade, product, or firms names is for descriptive purposes only and does not imply endorsement by the U.S. government.

References

Alward, R. D., J. K. Detling, and D. G. Milchunas, 1999: Grassland vegetation changes and nocturnal global warming. *Science,* **283,** 229–231, doi:10.1126/science.283.5399.229.

Angeles, M. E., J. E. Gonzalez, D. J. Erickson, and J. L. Hernández, 2007: Predictions of future climate change in the Caribbean region using global general circulation models. *Int. J. Climatol.,* **27,** 555–569, doi:10.1002/joc.1416.

Baldocchi, D., E. Falge, and K. Wilson, 2001: A spectral analysis of biosphere–atmosphere trace gas flux densities and meteorological variables across hour to multi-year time scales. *Agric. For. Meteor.,* **107,** 1–27, doi:10.1016/S0168-1923(00)00228-8.

Bayazit, M., and B. Önöz, 2007: To prewhiten or not to prewhiten in trend analysis? *Hydrol. Sci. J.,* **52,** 611–624, doi:10.1623/hysj.52.4.611.

Beck, H. E., L. A. Bruijnzeel, A. I. J. M. van Dijk, T. R. McVicar, F. N. Scatena, and J. Schellekens, 2013: The impact of forest regeneration on streamflow in 12 meso-scale humid tropical catchments. *Hydrol. Earth Syst. Sci. Discuss.,* **10,** 3045–3102, doi:10.5194/hessd-10-3045-2013.

Beniston, M., and M. Rebetez, 1996: Regional behavior of minimum temperatures in Switzerland for the period 1979–1993. *Theor. Appl. Climatol.,* **53,** 231–243, doi:10.1007/BF00871739.

Briscoe, C. B., 1966: Weather in the Luquilo Mountains of Puerto Rico. U.S. Department of Agriculture Forest Service Río Piedras Research Paper, 258 pp.

Buishand, T. A., 1978: Some remarks on the use of daily rainfall models. *J. Hydrol.,* **36,** 295–308, doi:10.1016/0022-1694(78)90150-6.

Burrowes, P. A., R. L. Joglar, and D. E. Green, 2004: Potential causes for amphibian declines in Puerto Rico. *Herpetologica,* **60,** 141–154, doi:10.1655/03-50.

Calvesbert, R. J., 1970: Climate of Puerto Rico and the US Virgin Islands. U.S. Department of Commerce Climatography of the United States 60-52, 451–478.

Campbell, J. D., M. A. Taylor, T. S. Stephenson, R. A. Watson, and F. S. Whyte, 2011: Future climate of the Caribbean from a regional climate model. *Int. J. Climatol.,* **31,** 1866–1878, doi:10.1002/joc.2200.

Cantrell, S. A., D. J. Lodge, C. A. Cruz, L. M. García, J. R. Pérez-Jiménez, and M. Molina, 2013: Differential abundance of microbial functional groups along the elevation gradient from the coast to the Luquillo Mountains. *Ecol. Bull.,* **54,** 87–100.

Cao, G., T. W. Giambelluca, D. E. Stevens, and T. A. Schroeder, 2007: Inversion variability in the Hawaiian trade wind regime. *J. Climate,* **20,** 1145–1160, doi:10.1175/JCLI4033.1.

Carter, M., and J. Elsner, 1997: A statistical method for forecasting rainfall over Puerto Rico. *Wea. Forecasting,* **12,** 515–525, doi:10.1175/1520-0434(1997)012<0515:ASMFFR>2.0.CO;2.

Coles, S., J. Bawa, L. Trenner, and P. Dorazio, 2001: *An Introduction to Statistical Modeling of Extreme Values.* Springer, 209 pp.

Comarazamy, D. E., and J. E. González, 2011: Regional long-term climate change (1950–2000) in the midtropical Atlantic and its impacts on the hydrological cycle of Puerto Rico. *J. Geophys. Res.,* **116,** D00Q05, doi:10.1029/2010JD015414.

Cox, D. R., and A. Stuart, 1955: Some quick sign tests for trend in location and dispersion. *Biometrika,* **42,** 80–95, doi:10.1093/biomet/42.1-2.80.

Curtis, S., 2002: Interannual variability of the bimodal distribution of summertime rainfall over Central America and tropical storm activity in the far-eastern Pacific. *Climate Res.,* **22,** 141–146, doi:10.3354/cr022141.

Denslow, J. S., 1987: Tropical rainforest gaps and tree species diversity. *Annu. Rev. Ecol. Syst.,* **18,** 431–451, doi:10.1146/annurev.es.18.110187.002243.

Dixon, W. J., 1950: Analysis of extreme values. *Ann. Math. Stat.,* **21,** 488–506, doi:10.1214/aoms/1177729747.

Dunham, J., G. Chandler, B. Rieman, and D. Martin, 2005: Measuring stream temperature with digital data loggers: A user's guide. U.S. Department of Agriculture Forest Service Rocky Mountain Research Station Rep., 18 pp.

Durre, I., Williams, C. N., Yin, X., and R. S. Vose, 2009: Radiosonde-based trends in precipitable water over the Northern Hemisphere: An update. *J. Geophys. Res.,* **114,** D05112, doi:10.1029/2008JD010989.

ElNesr, M. N., M. M. Abu-Zreig, and A. A. Alazba, 2010: Temperature trends and distribution in the Arabian Peninsula. *Amer. J. Environ. Sci.,* **6,** 191–203, doi:10.3844/ajessp.2010.191.203.

Enquist, C. A. F., 2002: Predicted regional impacts of climate change on the geographical distribution and diversity of tropical forests in Costa Rica. *J. Biogeogr.,* **29,** 519–534, doi:10.1046/j.1365-2699.2002.00695.x.

Ewel, J. J., and J. L. Whitmore, 1973: Ecological life zones of Puerto Rico and U.S. Virgin Islands. U.S. Forest Service Institute of Tropical Forestry, Research Paper ITF-018, 74 pp.

Fisher, R. A., and L. H. C. Tippett, 1928: Limiting forms of the frequency distribution of the largest or smallest member of a sample. *Math. Proc. Cambridge Philos. Soc.,* **24,** 180–190, doi:10.1017/S0305004100015681.

Foster, P., 2001: The potential negative impacts of global climate change on tropical montane cloud forests. *Earth-Sci. Rev.,* **55,** 73–106, doi:10.1016/S0012-8252(01)00056-3.

García-Martinó, A. R., G. S. Warner, F. N. Scatena, and D. L. Civco, 1996: Rainfall, runoff and elevation relationships in the Luquillo Mountains of Puerto Rico. *Caribb. J. Sci.,* **32,** 413–424.

Gelpi, C. G., and K. E. Norris, 2005: Seasonal and high-frequency ocean temperature dynamics at Santa Catalina Island. *Proc. Sixth California Islands Symp.,* Ventura, CA, National Park Service, 461–471.

Giambelluca, T. W., H. F. Diaz, and M. S. A. Luke, 2008: Secular temperature changes in Hawai'i. *Geophys. Res. Lett.,* **35,** L12702, doi:10.1029/2008GL034377.

Giannini, A., Y. Kushnir, and M. A. Cane, 2000: Interannual variability of Caribbean rainfall, ENSO, and the Atlantic Ocean. *J. Climate,* **13,** 297–311, doi:10.1175/1520-0442(2000)013<0297:IVOCRE>2.0.CO;2.

Giorgi, F., J. W. Hurrell, M. R. Marinucci, and M. Beniston, 1997: Elevation dependency of the surface climate change signal: A model study. *J. Climate,* **10,** 288–296, doi:10.1175/1520-0442(1997)010<0288:EDOTSC>2.0.CO;2.

González, G., and M. M. Luce, 2013: Woody debris characterization along an elevation gradient in northeastern Puerto Rico. *Ecol. Bull.,* **54,** 181–193.

Gouirand, I., M. R. Jury, and B. Sing, 2012: An analysis of low- and high-frequency summer climate variability around the Caribbean Antilles. *J. Climate,* **25,** 3942–3952, doi:10.1175/JCLI-D-11-00269.1.

Greenland, D., and T. G. Kittel, 2002: Temporal variability of climate at the US Long-Term Ecological Research (LTER) sites. *Climate Res.,* **19,** 213–231, doi:10.3354/cr019213.

Gumbel, E. J., 2012: *Statistics of Extremes.* Courier Dover, 402 pp.

Hall, T. C., A. M. Sealy, T. S. Stephenson, S. Kusunoki, M. A. Taylor, A. A. Chen, and A. Kitoh, 2013: Future climate of the Caribbean from a super-high-resolution atmospheric general circulation model. *Theor. Appl. Climatol.,* **113,** 271–287, doi:10.1007/s00704-012-0779-7.

Halpin, P. N., 1997: Global climate change and natural-area protection: Management responses and research directions. *Ecol. Appl.,* **7,** 828–843, doi:10.1890/1051-0761(1997)007[0828:GCCANA]2.0.CO;2.

Hamed, K. H., and A. R. Rao, 1998: A modified Mann-Kendall trend test for autocorrelated data. *J. Hydrol.,* **204,** 182–196, doi:10.1016/S0022-1694(97)00125-X.

Harris, N. L., and E. Medina, 2013: Changes in leaf properties across an elevation gradient in the Luquillo Mountains, Puerto Rico. *Ecol. Bull.,* **54,** 169–179.

Hartz, D. A., A. J. Brazel, and G. M. Heisler, 2006: A case study in resort climatology of Phoenix, Arizona, USA. *Int. J. Biometeor.,* **51,** 73–83, doi:10.1007/s00484-006-0036-9.

Heartsill-Scalley, T., F. N. Scatena, C. Estrada, W. H. McDowell, and A. E. Lugo, 2007: Disturbance and long-term patterns of rainfall and throughfall nutrient fluxes in a subtropical wet forest in Puerto Rico. *J. Hydrol.,* **333,** 472–485, doi:10.1016/j.jhydrol.2006.09.019.

Helsel, D. R., and L. M. Frans, 2006: Regional Kendall test for trend. *Environ. Sci. Technol.,* **40,** 4066–4073, doi:10.1021/es051650b.

Hilbert, D. W., B. Ostendorf, and M. S. Hopkins, 2001: Sensitivity of tropical forests to climate change in the humid tropics of north Queensland. *Austral Ecol.,* **26,** 590–603, doi:10.1046/j.1442-9993.2001.01137.x.

Hirsch, R. M., and J. R. Slack, 1984: A nonparametric trend test for seasonal data with serial dependence. *Water Resour. Res.,* **20,** 727–732, doi:10.1029/WR020i006p00727.

——, ——, and R. A. Smith, 1982: Techniques of trend analysis for monthly water quality data. *Water Resour. Res.,* **18,** 107–121, doi:10.1029/WR018i001p00107.

Hodson, D. L. R., R. T. Sutton, C. Cassou, N. Keenlyside, Y. Okumura, and T. Zhou, 2010: Climate impacts of recent multidecadal changes in Atlantic Ocean sea surface temperature: A multimodel comparison. *Climate Dyn.,* **34,** 1041–1058, doi:10.1007/s00382-009-0571-2.

Holdridge, L. R., W. C. Grenke, W. H. Hatheway, T. Liang, and J. A. Tosi, 1971: *Forest Environments in Tropical Life Zones: A Pilot Study.* Oxford, 747 pp.

Hughes, G. L., S. S. Rao, and T. S. Rao, 2007: Statistical analysis and time-series models for minimum/maximum temperatures in the Antarctic Peninsula. *Proc. Roy. Soc.,* **463A,** 241–259, doi:10.1098/rspa.2006.1766.

Jenkinson, A. F., 1955: The frequency distribution of the annual maximum (or minimum) values of meteorological elements. *Quart. J. Roy. Meteor. Soc.,* **81,** 158–171, doi:10.1002/qj.49708134804.

Jury, M. R., and I. Gouirand, 2011: Decadal climate variability in the eastern Caribbean. *J. Geophys. Res.,* **116,** D00Q03, doi:10.1029/2010JD015107.

Karmalkar, A. V., M. A. Taylor, J. Campbell, T. Stephenson, M. New, A. Centella, A. Benzanilla, and J. Charlery, 2013: A review of observed and projected changes in climate for the islands in the Caribbean. *Atmósfera,* **26,** 283–309.

Katz, R. W., 1977: Precipitation as a chain-dependent process. *J. Appl. Meteor.,* **16,** 671–676, doi:10.1175/1520-0450(1977)016<0671:PAACDP>2.0.CO;2.

Kendall, M. G., 1940: Note on the distribution of quantiles for large samples. *Suppl. J. Roy. Stat. Soc.,* **7,** 83–85, doi:10.2307/2983633.

Kendall, M. G., 1975: *Rank Correlation Methods.* Charles Griffin, 160 pp.

Larsen, M. C., and A. Simon, 1993: A rainfall intensity-duration threshold for landslides in a humid-tropical environment, Puerto Rico. *Geogr. Ann.,* **75A,** 13–23.

Li, Z., and Coauthors, 2012: Altitude dependency of trends of daily climate extremes in southwestern China, 1961–2008. *J. Geogr. Sci.,* **22,** 416–430, doi:10.1007/s11442-012-0936-z.

Liu, X., Z. Cheng, L. Yan, and Z.-Y. Yin, 2009: Elevation dependency of recent and future minimum surface air temperature trends in the Tibetan Plateau and its surroundings. *Global Planet. Change,* **68,** 164–174, doi:10.1016/j.gloplacha.2009.03.017.

Ljung, G. M., and G. E. P. Box, 1978: On a measure of lack of fit in time series models. *Biometrika,* **65,** 297–303, doi:10.1093/biomet/65.2.297.

Machiwal, D., and M. K. Jha, 2009: Time series analysis of hydrologic data for water resources planning and management: A review. *J. Hydrol. Hydromech.,* **54,** 237–257.

Mann, H. B., 1945: Nonparametric tests against trend. *Econometrica,* **13,** 245–259, doi:10.2307/1907187.

Martínez, M. D., C. Serra, A. Burgueño, and X. Lana, 2010: Time trends of daily maximum and minimum temperatures in Catalonia (ne Spain) for the period 1975–2004. *Int. J. Climatol.,* **30,** 267–290, doi:10.1002/joc.1884.

Medina, E., G. González, and M. M. Rivera, 2013: Spatial and temporal heterogeneity of rainfall inorganic ion composition in northeastern Puerto Rico. *Ecol. Bull.,* **54,** 157–167.

Méndez-Lázaro, P. A., A. Nieves-Santiango, and J. Miranda-Bermúdez, 2014: Trends in total rainfall, heavy rain events, and number of dry days in San Juan, Puerto Rico, 1955-2009. *Ecol. Soc.,* **19,** 50, doi:10.5751/ES-06464-190250.

Mielke, P. W., 1973: Another family of distributions for describing and analyzing precipitation data. *J. Appl. Meteor.,* **12,** 275–280, doi:10.1175/1520-0450(1973)012<0275:AFODFD>2.0.CO;2.

Murphy, S. F., and R. F. Stallard, 2012: Hydrology and climate of four watersheds in eastern Puerto Rico. Water quality and landscape processes of four watersheds in eastern Puerto Rico, S. F. Murphy and R. F. Stallard, Eds., U.S. Geological Survey Professional Paper 1789-C, 43–84.

Noether, G. E., 1948: On confidence limits for quantiles. *Ann. Math. Stat.,* **19,** 416–419, doi:10.1214/aoms/1177730209.

Partal, T., and E. Kahya, 2006: Trend analysis in Turkish precipitation data. *Hydrol. Processes,* **20,** 2011–2026, doi:10.1002/hyp.5993.

Pelletier, J. D., 2002: Natural variability of atmospheric temperatures and geomagnetic intensity over a wide range of time scales. *Proc. Natl. Acad. Sci. USA,* **99,** 2546–2553, doi:10.1073/pnas.022582599.

Phillips, O. L., and A. H. Gentry, 1994: Increasing turnover through time in tropical forests. *Science,* **263,** 954–958, doi:10.1126/science.263.5149.954.

Ping, C.-L., G. J. Michaelson, C. A. Stiles, and G. González, 2013: Soil characteristics, carbon stores, and nutrient distribution in eight forest types along an elevation gradient, eastern Puerto Rico. *Ecol. Bull.,* **54,** 67–86.

Prieto, G. A., R. L. Parker, D. J. Thomson, F. L. Vernon, and R. L. Graham, 2007: Reducing the bias of multitaper spectrum estimates. *Geophys. J. Int.,* **171,** 1269–1281, doi:10.1111/j.1365-246X.2007.03592.x.

Richards, M. T., M. L. Rogers, and D. S. P. Richards, 2009: Long-term variability in the length of the solar cycle. *Publ. Astron. Soc. Pac.,* **121,** 797–809, doi:10.1086/604667.

Richardson, B. A., and M. J. Richardson, 2013: Litter-based invertebrate communities in forest floor and bromeliad microcosms along an elevational gradient in Puerto Rico. *Ecol. Bull.,* **54,** 101–115.

——, ——, and F. N. Soto-Adames, 2005: Separating the effects of forest type and elevation on the diversity of litter invertebrate communities in a humid tropical forest in Puerto Rico. *J. Anim. Ecol.,* **74,** 926–936, doi:10.1111/j.1365-2656.2005.00990.x.

Riedel, K. S., and A. Sidorenko, 1995: Minimum bias multiple taper spectral estimation. *IEEE Trans. Signal Process.,* **43,** 188–195, doi:10.1109/78.365298.

Satterlund, D. R., R. C. Chapman, and R. D. Beach, 1983: Modeling the daily temperature cycle. *Northwest Sci.,* **57,** 22–31.

Scatena, F., 1998: An assessment of climate change in the Luquillo Mountains of Puerto Rico. *Proc. Third Int. Symp. on Water Resources,* San Juan, PR, American Water Resources Association, 193–198.

Schellekens, J., F. N. Scatena, L. A. Bruijnzeel, and A. J. Wickel, 1999: Modelling rainfall interception by a lowland tropical rain forest in northeastern Puerto Rico. *J. Hydrol.,* **225,** 168–184, doi:10.1016/S0022-1694(99)00157-2.

Scholl, M. A., and S. F. Murphy, 2014: Precipitation isotopes link regional climate patterns to water supply in a tropical mountain forest, eastern Puerto Rico. *Water Resour. Res.,* **50,** 4305–4322, doi:10.1002/2013WR014413.

Sen, P. K., 1968: Estimates of the regression coefficient based on Kendall's tau. *J. Amer. Stat. Assoc.,* **63,** 1379–1389, doi:10.1080/01621459.1968.10480934.

Serra, C., A. Burgueño, and X. Lana, 2001: Analysis of maximum and minimum daily temperatures recorded at Fabra Observatory (Barcelona, NE Spain) in the period 1917–1998. *Int. J. Climatol.,* **21,** 617–636, doi:10.1002/joc.633.

Shao, Q., and M. Li, 2011: A new trend analysis for seasonal time series with consideration of data dependence. *J. Hydrol.,* **396,** 104–112, doi:10.1016/j.jhydrol.2010.10.040.

Silver, W. L., D. Liptzin, and M. Almaraz, 2013: Soil redox dynamics and biogeochemistry along a tropical elevation gradient. *Ecol. Bull.,* **54,** 195–209.

Silverman, B. W., 1986: *Density Estimation for Statistics and Data Analysis.* CRC Press, 177 pp.

Smith, R. E., and H. A. Schreiber, 1974: Point processes of seasonal thunderstorm rainfall: 2. Rainfall depth probabilities. *Water Resour. Res.,* **10,** 418–423, doi:10.1029/WR010i003p00418.

Smith, R. L., 1989: Extreme value analysis of environmental time series: An application to trend detection in ground-level ozone. *Stat. Sci.,* **4,** 367–377, doi:10.1214/ss/1177012400.

Stephenson, T. S., and Coauthors, 2014: Changes in extreme temperature and precipitation in the Caribbean region, 1961–2010. *Int. J. Climatol.,* **34,** 2957–2971, doi:10.1002/joc.3889.

Still, C. J., P. N. Foster, and S. H. Schneider, 1999: Simulating the effects of climate change on tropical montane cloud forests. *Nature,* **398,** 608–610, doi:10.1038/19293.

Tayanç, M., and H. Toros, 1997: Urbanization effects on regional climate change in the case of four large cities of Turkey. *Climatic Change,* **35,** 501–524, doi:10.1023/A:1005357915441.

Taylor, M. A., D. B. Enfield, and A. A. Chen, 2002: Influence of the tropical Atlantic versus the tropical Pacific on Caribbean rainfall. *J. Geophys. Res.,* **107,** 3127, doi:10.1029/2001JC001097.

Thiel, H., 1950: A rank-invariant method of linear and polynomial regression analysis. *Proc. Nederl. Akad. Wetensch.,* **53,** 386–392.

Thom, H. C. S., 1952: Seasonal degree-day statistics for the United States. *Mon. Wea. Rev.,* **80,** 143–147, doi:10.1175/1520-0493(1952)080<0143:SDSFTU>2.0.CO;2.

Thompson, W. R., 1936: On Confidence ranges for the median and other expectation distributions for populations of unknown distribution form. *Ann. Math. Stat.,* **7,** 122–128, doi:10.1214/aoms/1177732502.

Todorovic, P., and D. A. Woolhiser, 1975: A stochastic model of *n*-day precipitation. *J. Appl. Meteor.,* **14,** 17–24, doi:10.1175/1520-0450(1975)014<0017:ASMODP>2.0.CO;2.

Torres-Valcárcel, Á. R., J. Harbor, A. L. Torres-Valcárcel, and C. J. González-Avilés, 2014: Historical differences in temperature between urban and non-urban areas in Puerto Rico. *Int. J. Climatol.,* doi:10.1002/joc.4083, in press.

Valdez-Cepeda, R. D., A. A. Aguilar-Campos, F. Blanco-Macías, G. M. de León, S. de Jesús Méndez-Gallegos, and R. Magallanes-Quintanar, 2012: Analysis of precipitation in central México: Trends, self-affinity and important frequencies. *Int. J. Phys. Sci.,* **7,** 5324–5326, doi:10.5897/IJPS12.421.

van Belle, G., and J. P. Hughes, 1984: Nonparametric tests for trend in water quality. *Water Resour. Res.,* **20,** 127–136, doi:10.1029/WR020i001p00127.

Vitousek, P. M., 1998: The structure and functioning of montane tropical forests: control by climate, soils, and disturbance. *Ecology,* **79,** 1–2, doi:10.1890/0012-9658(1998)079[0001:TSAFOM]2.0.CO;2.

Vose, R. S., D. R. Easterling, and B. Gleason, 2005: Maximum and minimum temperature trends for the globe: An update through 2004. *Geophys. Res. Lett.,* **32,** L23822, doi:10.1029/2005GL024379.

Waide, R. B., and Coauthors, 2013: Climate variability at multiple spatial and temporal scales in the Luquillo Mountains, Puerto Rico. *Ecol. Bull.,* **54,** 21–41.

Wang, H., C. A. S. Hall, F. N. Scatena, N. Fetcher, and W. Wu, 2003: Modeling the spatial and temporal variability in climate and primary productivity across the Luquillo Mountains, Puerto Rico. *For. Ecol. Manage.,* **179,** 69–94, doi:10.1016/S0378-1127(02)00489-9.

Weaver, P. L., 1972: Cloud moisture interception in the Luquillo Mountains of Puerto Rico. *Caribb. J. Sci.,* **12,** 129–144.

——, and P. G. Murphy, 1990: Forest structure and productivity in Puerto Rico's Luquillo Mountains. *Biotropica,* **22,** 69–82, doi:10.2307/2388721.

——, and W. A. Gould, 2013: Forest vegetation along environmental gradients in northeastern Puerto Rico. *Ecol. Bull.,* **54,** 43–65.

Wilks, S. S., 1948: Order statistics. *Bull. Amer. Math. Soc.,* **54,** 6–50, doi:10.1090/S0002-9904-1948-08936-4.

Willig, M. R., S. J. Presley, C. P. Bloch, and J. Alvarez, 2013: Population, community, and metacommunity dynamics of terrestrial gastropods in the Luquillo Mountains: A gradient perspective. *Ecol. Bull.,* **54,** 117–140.

Woolhiser, D. A., and G. G. S. Pegram, 1979: Maximum likelihood estimation of Fourier coefficients to describe seasonal variations of parameters in stochastic daily precipitation models. *J. Appl. Meteor.,* **18,** 34–42, doi:10.1175/1520-0450(1979)018<0034:MLEOFC>2.0.CO;2.

Wu, W., M. A. Geller, and R. E. Dickinson, 2002: The response of soil moisture to long-term variability of precipitation. *J. Hydrometeor.,* **3,** 604–613, doi:10.1175/1525-7541(2002)003<0604:TROSMT>2.0.CO;2.

Yue, S., and C. Wang, 2004: The Mann-Kendall test modified by effective sample size to detect trend in serially correlated hydrological series. *Water Resour. Manage.,* **18,** 201–218, doi:10.1023/B:WARM.0000043140.61082.60.

——, P. Pilon, B. Phinney, and G. Cavadias, 2002: The influence of autocorrelation on the ability to detect trend in hydrological series. *Hydrol. Processes,* **16,** 1807–1829, doi:10.1002/hyp.1095.

Zalamea, M., and G. González, 2008: Leaffall phenology in a subtropical wet forest in Puerto Rico: From species to community patterns. *Biotropica,* **40,** 295–304, doi:10.1111/j.1744-7429.2007.00389.x.

Zhang, G. P., and M. Qi, 2005: Neural network forecasting for seasonal and trend time series. *Eur. J. Oper. Res.,* **160,** 501–514, doi:10.1016/j.ejor.2003.08.037.

Zhang, X., and F. W. Zwiers, 2004: Comment on "Applicability of prewhitening to eliminate the influence of serial correlation on the Mann-Kendall test" by Sheng Yue and Chun Yuan Wang. *Water Resour. Res.,* **40,** W03805, doi:10.1029/2003WR002073.

Earth Interactions is published jointly by the American Meteorological Society, the American Geophysical Union, and the Association of American Geographers. Permission to use figures, tables, and *brief* excerpts from this journal in scientific and educational works is hereby granted provided that the source is acknowledged. Any use of material in this journal that is determined to be "fair use" under Section 107 or that satisfies the conditions specified in Section 108 of the U.S. Copyright Law (17 USC, as revised by P.IL. 94-553) does not require the publishers' permission. For permission for any other from of copying, contact one of the copublishing societies.